# Dangerous degree forecast of soil loss on highway slopes in mountainous areas of Yunnan–Guizhou Plateau (China) using the Revised Universal Soil Loss Equation

**Yue Li[1,2], Shi Qi*[1,2], Bin Liang[1,2], Junming Ma[1,2], Baihan Cheng[1,2], Cong Ma[3], Yidan Qiu[3], and Qinyan Chen[3]**

[1] Key Laboratory of State Forestry Administration on Soil and Water Conservation, Beijing Forestry University, Beijing 100083, China

[2] Beijing Engineering Research Center of Soil and Water Conservation, Beijing Forestry University, Beijing 100083, China

[3] Yunnan Science Research Institute of Communication & Transportation, Kunming 650011, China

**Abstract**

Many high and steep slopes are formed by special topographic and geomorphic types and mining activities during the construction of mountain expressways. Severe soil erosion may also occur under heavy rainfall conditions. Therefore, predicting soil loss on highway slopes is important in protecting infrastructure and human life. In this study, we investigate Xinhe Expressway located at the southern edge of the Yunnan–Guizhou Plateau. The revised universal soil loss equation is used as the prediction model for soil and water loss on slopes. Geographic information systems, remote sensing technology, field surveys, runoff plot observation testing, cluster analysis and co-kriging calculations are also utilised. The partition of the prediction units of soil loss on the expressway slope in the mountainous area and the spatial distribution of rainfall on a linear highway are studied. Given the particularity of the expressway slope in the mountainous area, the model parameter is modified, and the risk of soil loss along the mountain expressway is simulated and predicted under 20- and 1-year rainfall return periods. The following results are obtained. (1) Natural watersheds can be considered for the prediction of slope soil erosion to represent the actual situation of soil loss on each slope. Then, the spatial location of the soil erosion unit can be determined. (2) Analysis of actual observation data shows that the overall average absolute error of the monitoring area is 0.39 $t \cdot ha^{-1}$, the overall average relative error is 33.96% and the overall root mean square error is between 0.21 and 0.66, all of which are within acceptable limits. The Nash efficiency coefficient is 0.67, indicating that the prediction accuracy of the model satisfies the requirements. (3) Under the 1-year rainfall return period condition, we find through risk classification that the percentage of prediction units with no risk of erosion is 78%. The soil erosion risk is low and does not affect road traffic safety. Under the 20-year return period rainfall condition, the percentage of units with high and extremely high risks is 7.11%. The

prediction results can help adjust the design of water and soil conservation measures for these units.

**Keywords:** Soil loss; highway slopes; mountainous areas; RUSLE; dangerous degree forecast

## Introduction

China has gradually accelerated its construction of highways in recent years, improved its transportation networks and promoted rapid economic development (Jia et al., 2005). With the implementation of the Western development strategy, advanced requirements for the construction of expressways have been proposed to connect coastal plains and inland mountains. However, many unstable high and steep slopes, such as natural, excavation and fill slopes, are inevitably formed by the frequent filling and deep digging along expressways in mountain areas.

The slope is the most fragile part of an expressway in a mountain area. During rainy seasons, soil erosion is easily caused by rainwash and leads to considerable damage (Figure 1). At present, China's highway industry remains in a period of rapid development. At the end of 2017, the total mileage of road exceeded 4,773,500 km, whilst that of highways was 136,500 km (china. com. cn., 2018; Mori et al., 2017; Kateb et al., 2013; Zhou et al., 2016). Statistics further indicate that in the next 20–30 years, the expressways in China will have a total length of more than 40,000 km. For every kilometre of highway, the corresponding bare slope area is expected to reach 50,000–70,000 $m^2$ (Wang, 2006). The annual amount of soil erosion is 9,000 $g/m^3$, which can cause 450 t of soil loss annually (Chen, 2010). The soil loss of roadbed slopes differs from the soil loss in woodlands and farmlands. Forestlands and farmlands are generally formed after years of evolution and belong to the native landscape. Most of the slopes of these land types are gentle and stable (Kateb et al., 2013). Moreover, traditional soil and water conservation research has focused on slopes with 20% grade or below, but roadbed slopes of highways generally have a grade of 30% or above (Zhou, 2010). Soil erosion on roadbed side slopes affects not only soil loss along highways but also road operation safety (Gong and Yang, 2016; Jiang et al., 2017). Therefore, soil erosion on the side slopes of mountain expressways must be studied to control soil erosion, improve the ecological environment of expressways and realise sustainable land utilisation (Wang et al., 2005; Yang and Wang, 2006).

The revised universal soil loss equation (RUSLE) is a set of mathematical equations used to estimate the average annual soil loss and sediment yield resulting from inter-rill and rill erosion (Renard et al., 1997; Foster et al., 1999; Zerihun et al., 2018; Toy et al., 2002). RUSLE was derived from the theory of erosion processes and has been applied to more than 10,000 plot-years of data from natural rainfall plots and numerous rainfall-simulation plots. RUSLE is an exceptionally well-validated and documented equation. It was conceptualised by a group of nationally recognised scientists and soil conservationists with extensive experience in erosion

processes (Soil and Water Conservation Society, 1993).

The use of RUSLE models as predictive tools for the quantitative estimation of soil erosion has matured (Panagos et al., 2018; Cunha et al., 2017; Taye et al., 2017; Renard, 1997). The range of application of these models involves nearly every aspect of soil erosion. Moreover, many scientists have conducted useful explorations to modify the model's parametric values and improve its simulation accuracy.

Tresch et al. (1995), in a study in Switzerland, argued that slope length (*L*) and slope steepness (*S*) are crucial factors in soil erosion prediction, and these parameters significantly influence the erosion values calculated by RUSLE. All existing *S* factors can be derived only from gentle slope inclinations of up to 32%; however, many cultivated areas are steeper than this critical value. A previous study used 18 plot measurements on transects along slopes with steepness from 20% to 90% to qualitatively assess the most suitable *S* factors for steep subalpine slopes; the results showed that the first selection of the *S* factor is possible for slopes beyond the critical steepness of 25% (Tresch et al., 1995). Rick et al. (2001) found that using universal soil loss equation (USLE) and RUSLE soil erosion models at regional landscape scales is limited by the difficulty of obtaining an *LS* factor grid suitable for geographic information system (GIS) applications. Therefore, their modifications were applied to the previous arc macro language (AML) code to produce a RUSLE-based version of the *LS* factor grid. These alterations included replacing the USLE algorithms with their RUSLE counterparts and redefining the assumptions on slope characteristics. In areas of western USA where the models were tested, the RUSLE-based AML program produced *LS* values that were roughly comparable to those listed in the RUSLE handbook guidelines (Rick et al., 2001). Silburn (2011) showed that estimating the soil erodibility factor (*K*) from soil properties (derived from cultivated soils) provides a reasonable estimate of *K* for the main duplex soils at the study site as long as the correction for undisturbed soil is used to derive K from the measured data before application to the USLE model (Silburn, 2011). Wu (2014) adopted GIS and RUSLE methods to analyse the risk pattern of soil erosion in the affected road zone of Hangjinqu Highway in Zhuji City, Zhejiang Province. Digital elevation model (DEM) data, rainfall records, soil type data, remote sensing imaging and a road map of Hangjinqu Highway were used for GIS and RUSLE analyses (Wu et al., 2014). Chen (2010), who initially considered the terrain characteristics of roadbed side slopes and conducted a concrete analysis of the terrain factor calculation method in RUSLE, evaluated a compatible terrain factor computational method of roadbed side slopes and proposed a revised method based on the measured data of soil erosion in the subgrade side slope of Hurongxi Expressway (from Enshi to Lichuan) in Hubei Province. The results indicated that (1) the slope length factor in RUSLE can be calculated by $L=\left(\lambda/22.1\right)^{m}$, but *m* should not be computed by using the original method for highway subgrade side slope because its gradient surpasses the generally applicable scope of RUSLE. Moreover, (2) the slope length factor (*L*) of the highway subgrade side slope can be

calculated by $L=\left(\lambda/22.1\right)^{0.35}$ (Chen et al., 2010). Zhang (2016) investigated the spatiotemporal distribution of soil erosion in a ring expressway before and after construction by using a land use/cover map of Ningbo City in 2010. The topographic map of the North Ring Expressway and field survey data were collected for the DEM. Rainfall data were also collected from local hydrological stations. On the basis of the collected data, the spatial distribution of the factors in the RUSLE model was calculated, and soil erosion maps of the North Ring Expressway were estimated. Then, the soil erosion amount was calculated at three different stages by RUSLE. The results showed that slight erosion was dominant during the preconstruction and natural recovery periods, which accounted for 98.53% and 99.73%, respectively. During the construction period, mild erosion and slight erosion had the largest values and accounted for 52.5% and 35.4%, respectively. Soil erosion during the construction period was mainly distributed in temporary ground soil (Zhang et al., 2016).

However, the common methods used to fit the parameters can affect the findings, and minimising the sum of the squares of errors for soil loss may provide better results than simply fitting an exponential equation. Yang (2014) found that the *C* factor, as a function of fractional bare soil and ground cover, can be derived from MODIS data at regional or catchment scales. The method offered a meaningful estimate of the *C* factor for determining ground cover impact on soil loss and erosion hazard areas. The method performed better than commonly used techniques based on green vegetation only (e.g. normalised difference vegetation index (NDVI)), and it was appropriate for estimating the vegetation cover management factor (*C*) in the modelled hillslope erosion in New South Wales, Australia by using emerging fractional vegetation cover products. Moreover, the approach effectively mapped the spatiotemporal distribution of the RUSLE cover factor and the hillslope erosion hazard in a large area. The methods and results described in this previous work are important in understanding the spatiotemporal dynamics of hillslope erosion and ground cover. According to Kinnell (2014), runoff production, which is spatially uniform, is often inappropriate under natural conditions because infiltration is spatially variable. Upslope length varies with the ratio of the upslope runoff coefficient to the runoff coefficient for the area below the downslope boundary of the segment in the modified RUSLE approach. The use of upslope length produces only minor variations in soil loss compared with using values predicted by the standard RUSLE approach when the runoff is spatially variable and the number of segments increases. By contrast, the USLE-M approach can predict soil loss that is influenced strongly by runoff when runoff varies in space and time. Therefore, an increase in runoff through a segment causes an increase in soil loss, and a decrease in runoff through a segment or cell results in a decrease in soil loss.

In general, past studies (e.g. Tresch et al., 1995; Rick et al., 2001; Silburn, 2011; Yang, 2014; Kinnell, 2014) focused on sloping fields, but the research on soil erosion on highway slopes is limited. Subgrade slope is a major part of soil erosion during construction and operation periods.

Therefore, soil erosion caused by subgrade slope should be predicted. However, the research on soil loss of highways hardly meets the requirements of practical work (Xu et al., 2009; Bakr et al., 2012). We still need to conduct considerable work on the prediction of soil erosion on highway slopes. The situation in various regions in China indicates that researchers have helped improve the RUSLE model and studied soil erosion in certain areas. Water and soil erosion caused by engineering construction is an important aspect of research, especially from the perspective of agricultural cultivation and forestry deforestation, because the amount of eroded soil produced by embankment slopes accounts for a large proportion of the entire project area. Although this concern is related to project feasibility and cost in particular, the topic has elicited considerable interest in general. Furthermore, the principal factor that causes soil erosion on slopes generally corresponds to precipitation amount and embankment width. Wang (2005) established several experimental standardised spots for soil loss collection on the side slopes of the Xiaogan–Xiang Fan Freeway (i.e. under construction thus far) and installed an on-the-spot rainfall auto-recorder. The collected data were used for the revision of the main parameters *R* (rainfall and runoff) and *K* (erodibility of soil) of USLE, which is widely applied to forecast soil loss quantity in plowlands and predict the soil loss quantities of different types of soil on side slopes disturbed by engineering treatments (Wang et al., 2005). This method not only applies to the prediction of disturbed soil loss during expressway construction but also improves prediction accuracy. It also provides scientific support for relevant units or personnel to implement reasonable preventive measures.

Related literature indicates that research on soil loss in highways has the following limitations. First, most of the studies on *C* and *P* factors that used the RUSLE model were conducted by referring to previous research results, and data accuracy is often poor. Second, most studies on rainfall erosivity (*R*) factors are limited to sloping fields, and the rainfall erosivity factors of expressway slopes in mountain areas have rarely been studied. Third, slope soils in highways differ depending on soil arability, and the slopes also vary. Thus, accurately predicting the soil loss of different types of subgrade slopes by using the traditional *K* factor calculation method is difficult.

Previous studies have shown that the spatial interpolation method of precipitation is unsuitable for the study of the spatiotemporal distribution of precipitation in mountain areas (Liu and Zhang, 2006). The problem involves two aspects. From the timescale perspective, the characteristics of rainfall distribution and the influencing factors are not fully considered. From the spatial scale perspective, the spatial heterogeneity of the region is ignored. Furthermore, many studies have limited the factors that affect precipitation to altitude factors, leading to low interpolation accuracy (Zhao et al., 2011; Liu et al., 2010). Thus, in this study, we consider the spatial heterogeneity of linear engineering of the expressway. The rainfall factor is spatially interpolated to compensate for the following limitations: shortage of rainfall data on mountain areas, difficulty of representing the rainfall data of an entire expressway by using data from a single meteorological station, and uneven spatial distribution and strong heterogeneity of rainfall

in mountain areas (Li et al., 2017). We analyse the characteristics of soil erosion to improve certain aspects of expressway construction on the basis of previous research. We divide a highway slope into natural and artificial units and calculate the amount of soil loss from the slope surface to the pavement based on the slope surface catchment unit. The findings can be popularised because this approach is in line with the actual situation. Next, we modify the parameters of the artificial slope through an actual survey, runoff plot observation and other methods, and the parameters of the artificial slope are corrected by referring to the form of the project and the utilised materials. We not only scientifically predict the amount of soil erosion caused by highway construction in mountain areas but also provide a scientific basis for the prevention and control of soil erosion and rational allocation of prevention and control measures. The safe operation of highways and the virtuous cycle of the ecological environment should be ensured to promote the sustainable development of the local economy.

## 1 Study area

Xinhe Expressway is in the southern margin of the Yunnan–Guizhou Plateau, which is in southeast Yunnan Province, Honghe Prefecture and Hekou County. This highway was the first in Yunnan to cross the border. Thus, it has become an important communication channel between China and Vietnam and possesses an important strategic and economic value. The highway is at longitude 103° 33′ 45″–103° 58′ 32″ and latitude 22° 31′ 19″–22° 51′ 48″ (Figure 2) The expressway stretches roughly from northwest to southeast, and its total length is 56.30 km. The climate type belongs to subtropical mountain, seasonal monsoon forest and humid heat climate categories. Between May and the middle of October, the area experiences wet season characterised by abundant rainfall, concentrated precipitation and increased rain at night time; the variation of precipitation is 400–2000 mm, whilst most regions have 800–1800 mm (Fei et al., 2017; Zhang et al., 2017). During the rest of the year, the area undergoes dry season. The starting point of Xinhe Expressway is in Hekou County, New Street (pile number K83+500), at an altitude of 296 m. The endpoint is in the estuary of Areca Village (pile number K139+800) at an altitude of 95 m. The mountains along both sides are 200–380 m above sea level. The topography of the hilly area in the northern part of Xinhe Expressway is complicated. The slopes on both sides rise and fall, and most of the valleys constitute V- and U-shaped sections. The natural slopes on both sides are mostly below 57.7%. The southern part of the highway has a relatively flat terrain and a gentle slope. The slopes of most hills on both sides are less than 26.8%, and the overall height difference is less than 100 m. The vegetation in the southern part of Xinhe Expressway includes tropical rainforests and tropical monsoon forests, whilst that in the northern part of China is classified as south subtropical monsoon evergreen broad-leaved forest. In recent years, the original vegetation in this area has been reclaimed as farmland and is now planted with rubber, banana, pineapple and pomegranate, which are sporadic tropical rainforest survivors. The project area along Xinhe Expressway is an economic forest belt with a single vegetation type and mainly has rubber, forest

and other economic trees. The soil types along the highway are rich and mainly comprise red, leached cinnamon, grey forest and grey cinnamon soils.

**Figure 1.** Soil erosion produced by rainwash on a slope after rainfall

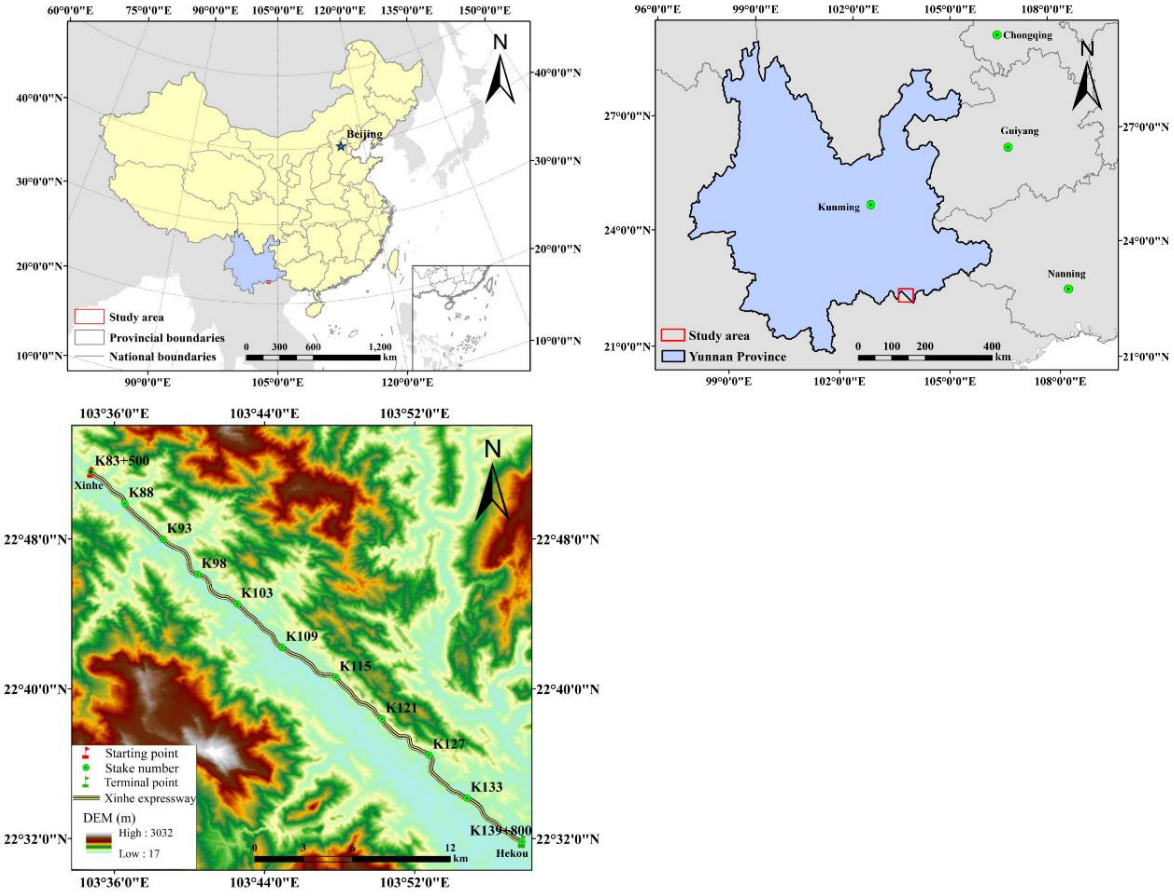


Figure 2. The location and the overview of the study region

## 2 Materials and methods

### 2.1 Data sources

Rainfall data from 2014 were obtained from Hekou Yao Autonomous County, Pingbian Miao Autonomous County, Jinping Miao Yao Autonomous County and the meteorological department of Mengzi. The rainfall data were obtained at 5 min intervals. Meanwhile, two automatic weather stations were established along Xinhe Expressway to gather weather data during the 2014 experiment. Meteorological data, which were provided by the China Meteorological Data Network, covered the period of 1959–2015 (http://data.cma.cn/site/index.html).

Data on soil types were provided by Yunnan Traffic Planning and Design Institute. Data on soil texture and organic matter were obtained via field surveys, data sampling and processing methods. Soil samples were initially collected at each 1 km range of the artificial and natural slopes on both sides of the highway. Five mixed soil samples were obtained from one slope by using the 'S'-shaped sampling method (Shu et al., 2017). Then, the method of coning and quartering was adopted (Oyekunle et al., 2011), and half of the mixed soil samples were brought to the laboratory for analysis. Finally, 186 soil samples were obtained. After the soil samples were dried and sieved, soil texture and organic carbon content were measured via specific gravity speed measurement and potassium dichromate external heating, respectively.

The topographic map and design drawings of Xinhe Expressway were provided by the Traffic Planning and Design Institute of Yunnan Province. The 1:2000 scale of the topographic map coordinate system was based on the 2000 GeKaiMeng urban coordinate system, the elevation system for 1985 national height data and the format for the CAD map in DWG. The remote sensing images used in this study were derived from 8 m hyperspectral images produced by the GF-1 satellite (http://www.rscloudmart.com/).

### 2.2 Prediction model selection

The RUSLE equation (Renard et al., 1997) was used to predict soil and water loss on the side slopes of Xinhe Expressway. The RUSLE equation considers natural and anthropogenic factors that cause soil erosion to produce comprehensive results. The parameters are easy to calculate, and the calculation method is relatively mature. The RUSLE model is suitable for soil erosion prediction in areas where physical models are not required. Formula (1) is expressed as

$$A = R \cdot K \cdot L \cdot S \cdot C \cdot P, \quad (1)$$

where $A$ is the average soil loss per unit area by erosion ($t \cdot ha^{-1} \cdot yr^{-1}$), $R$ is the rainfall erosivity factor (MJ·mm / (ha·h·yr)), $K$ is the soil erodibility factor (t·ha·h / (ha·MJ·mm)), $L$ is the slope length factor, $S$ is the steepness factor, $C$ is the cover and management practice factor and $P$ is the

conservation support practice factor. The values of $L$, $S$, $C$ and $P$ are dimensionless.

### 2.3 Division and implementation of the prediction unit

Geological structures and rock and soil categories are complex because of considerable changes in topography and physiognomy. The forms of slopes also vary. In general, according to the relationship between slope and engineering, slopes can be natural or artificial. Artificial slope formations can be subdivided into slope embankments and cutting slopes. In this study, we used ArcGIS software to convert the topographic map of the highway design into a vectorisation file because the artificial and natural slopes of watershed catchments are the main components of soil erosion prediction. On the basis of the extracted graphical units, the natural and artificial slopes were divided into uniform prediction units according to aspect, slope, land use and water conservation measures. The aspect, slope, land use, water conservation measures and other attributes of each prediction unit were consistent.

## 3 Results and analysis

### 3.1 Natural slope catchment area

The catchment unit of the slope was initially constructed by using the structural plane tools of ArcGIS combined with ridge and valley lines and artificial slope and highway boundaries (Zerihun et al., 2018). After the completion of the catchment unit, the slope was divided according to soil type data (Table 1). After the division and overlaying of the remote sensing image map, the land use types and soil and water conservation measures were considered as indicators for the visual interpretation of the field survey results and for further classification of the confluence units. The partition units were amended by using the vegetation coverage data obtained along Xinhe Expressway. A total of 814 natural slope catchment prediction units were divided.

**Table 1.** Distribution of soil types along Xinhe Expressway

| Section of the expressway | Soil type |
|---|---|
| K83+500~K84+900 | latosolic red soil |
| K85+200~K93+200 | leached cinnamon soil |
| K93+200~K95+900 | grey forest soil |
| K96+900~K97+800 | grey cinnamon soil |
| K97+800~K100+500 | leached cinnamon soil |

| | |
|---|---|
| K100+500~K101+100 | grey cinnamon soil |
| K101+100~K104 | leached cinnamon soil |
| K104~K109+100 | grey cinnamon soil |
| K109+100~K139 | leached cinnamon soil |

The artificial slope was divided into roadbed and cutting slopes according to the design of Xinhe Expressway (i.e. 1:1.5 and 1:1.0 slopes). After the preliminary division, the slope measurements, data design and field survey results were used as a basis for the subsequent detailed division of the artificial slope into cement frame protection and six arris brick revetments. McCool (1987) stated that slope length can vary within a 10 m range and only has a small effect on results. The specifications of each frame in the cement frame protection along Xinhe Expressway were the same. The horizontal projection length of a cement frame can be regarded the slope length value of an artificial slope. Therefore, the slope length of the artificial slope of each frame of the cement revetment was considered the same, and the value was set to 0. According to investigations, the vegetation coverage of artificial slopes with different plant species varies substantially. To achieve an accurate prediction of unit division and improve prediction accuracy, the artificial slopes should be continuously classified according to plant species. Thus, 422 artificial slope prediction units were obtained. The data of the 1236 slope prediction units were edited by using GIS. The results are shown in Figure 3.

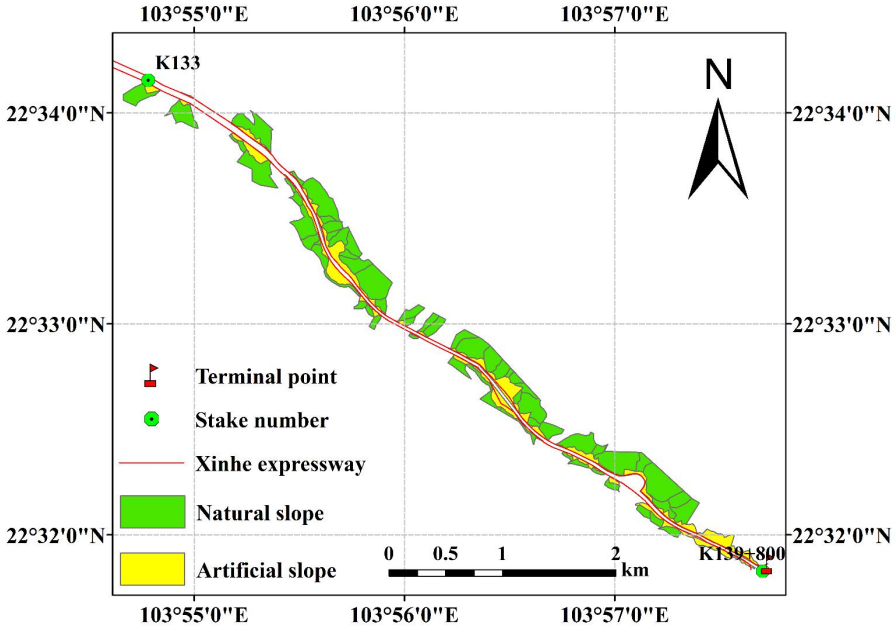


**Figure 3.** Division results of the prediction units (A subset-6.8 km)

## 3.2 Determination of conventional parameters of the RUSLE model

303 3.2.1 Rainfall erosivity factor ($R$)

304 The formula of the $R$-value (rainfall erosivity) was adopted (Wang et al., 1995; Liu et al.,
305 1999; Yang et al., 1999; Panagos et al., 2017) and calculated by using 30 min rainfall intensity as
306 the measure, as shown in Formulas (2) and (3).

307 $$R = 1.70 \cdot (P \cdot I_{30} / 100) - 0.136 \qquad (I_{30} < 10\ mm/h), \tag{2}$$

308 $$R = 2.35 \cdot (P \cdot I_{30} / 100) - 0.523 \qquad (I_{30} \geq 10\ mm/h), \tag{3}$$

309 where $R$ is rainfall erosivity (MJ·mm / (ha·h)), $P$ is sub-rainfall (mm) and $I_{30}$ is the maximum 30-
310 minitue intensity of the storm (mm·h$^{-1}$).

311 Rainfall data were acquired from stationary ground meteorological stations. However, using
312 data from a single meteorological station to represent the rainfall data of a linear mountain
313 expressway is difficult. The $P$ and $I_{30}$ values along the highway were obtained by co-kriging
314 calculations. The dataset included the following: rainfall data; 30 min rainfall data from the four
315 meteorological stations in Hekou Yao Autonomous County, Pingbian Miao Autonomous County,
316 Jinping Miao Yao Autonomous County and Mengzi City; and data acquired from two automatic
317 weather stations along the highway. Then, the cross-validation method was used to evaluate the
318 accuracy of the interpolation results. The selection criteria included the standard root mean square
319 error and the mean standard error. The detailed results are shown in Table 2. However, this work
320 shows only the interpolated results of secondary rainfall of two rainfall events and the 30 min
321 rainfall intensity data, as shown in Figures 4(a) and 4(b).

322 **Table 2.** Interpolation error of $P$ and $I_{30}$ values

| The time of storm event or rainfall event | $P$ | | $I_{30}$ | |
|---|---|---|---|---|
| | RMSS | MS | RMSS | MS |
| 2014.06.05 | 1.02 | -0.02 | 1.06 | -0.05 |
| 2014.06.07 | 1.04 | -0.02 | 1.01 | 0.02 |
| 2014.06.17 | 1.09 | 0.03 | 1.11 | 0.06 |
| 2014.06.28 | 1.11 | 0.07 | 1.05 | -0.03 |
| 2014.07.01 | 1.10 | 0.04 | 1.06 | -0.04 |
| 2014.07.13 | 1.03 | -0.02 | 1.01 | 0.02 |
| 2014.07.20 | 1.01 | 0.01 | 1.05 | 0.02 |

| | | | | |
|---|---|---|---|---|
| 2014.08.02 | 1.03 | 0.03 | 0.94 | 0.02 |
| 2014.08.12 | 1.05 | -0.03 | 1.10 | 0.03 |
| 2014.08.26 | 1.03 | 0.01 | 0.97 | 0.03 |
| 2014.08.29 | 1.09 | -0.02 | 1.03 | -0.02 |
| 2014.09.02 | 1.07 | 0.03 | 1.05 | 0.02 |
| 2014.09.04 | 0.96 | -0.02 | 0.97 | -0.02 |
| 2014.09.17 | 1.07 | -0.03 | 1.09 | -0.03 |
| 2014.09.20 | 0.98 | 0.05 | 1.03 | 0.02 |
| 2014.10.05 | 1.02 | 0.03 | 1.04 | 0.03 |

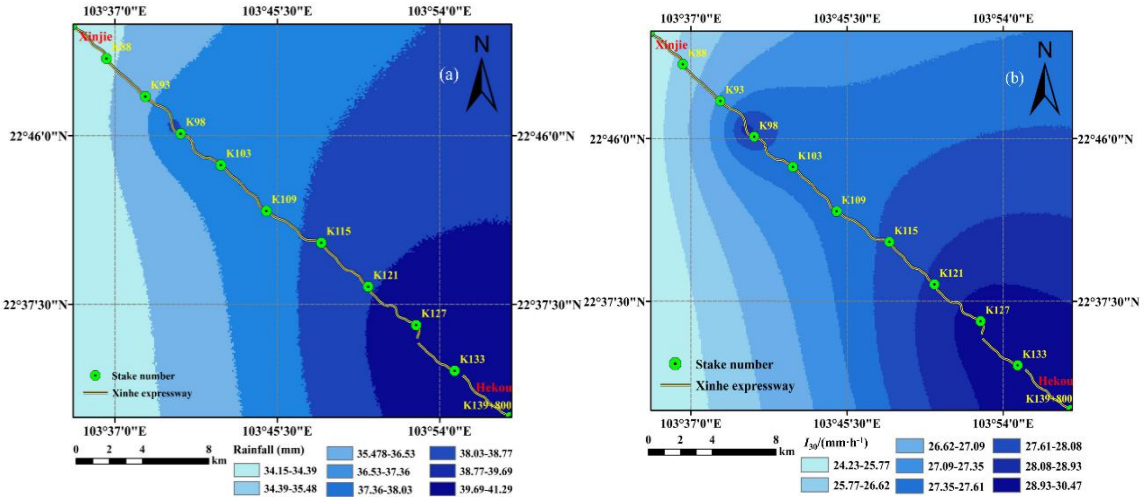


**Figure 4(a).** Interpolation results of secondary rainfall for June 5, 2014

**Figure 4(b).** Interpolation results of $I_{30}$ for June 5, 2014

The secondary rainfall data of 16 rainfall instances along Xinhe Expressway were obtained by interpolation because the values for internal rainfall and the rainfall intensity of a single prediction unit are the same. Therefore, the *R*-value was calculated by using the average rainfall and rainfall intensity of the unit. Only the spatial distribution map of the rainfall erosivity factors in certain sections (June 5, 2014) is shown because of space constraints (Figures 5 and 6).

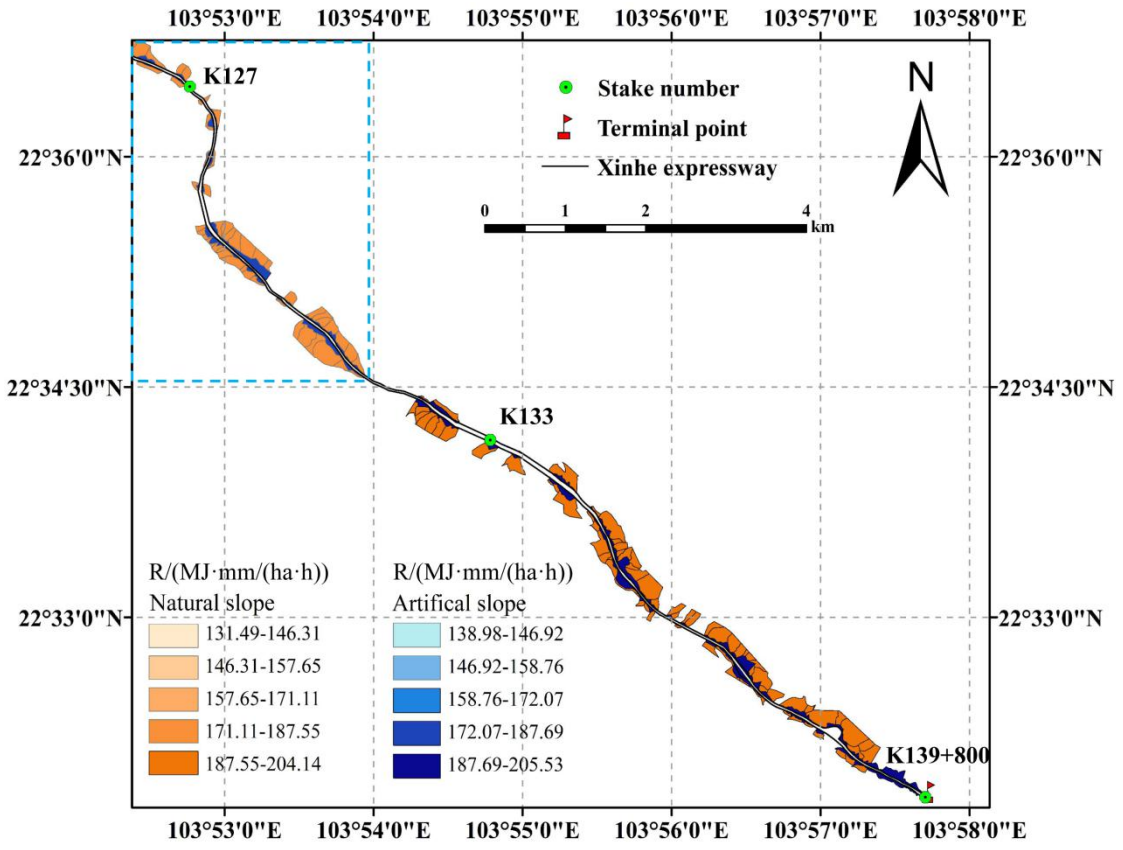


**Figure 5.** Spatial distribution map of rainfall erosivity factors (K127–K139+800)

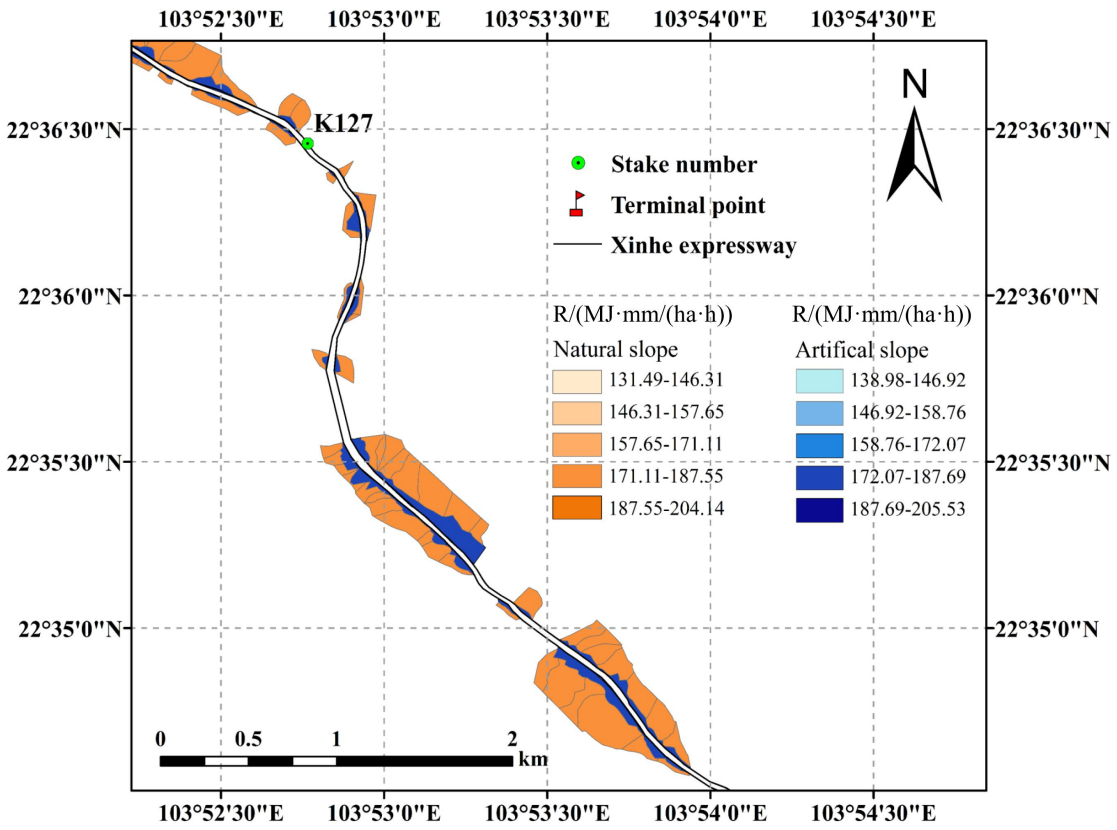


**Figure 6.** Spatial distribution of rainfall erosion factor in typical a section of a highway

336 3.2.2 Soil erodibility factor (*K*)

337 The soil data of a slope in each section were obtained by sampling according to the spatial
338 distribution map of soil types in the study area and by dividing the linear distribution of the soil.
339 The *K* value was calculated by applying Formula 4 to obtain the soil erodibility factor values of
340 each slope (Sharply and Williams, 1990) (Tables 3 and 4; see supplementary material/appendices).

341 $$K = 0.2 + 0.3e^{[0.0256SAN(1-SIL/100)]} \times \left(\frac{SIL}{CLA+SIL}\right)^{0.3} \times \left[1 - \frac{0.25C}{C + e^{3.72-2.95C}}\right] \times \left[1 - \frac{0.75N_1}{SN_1 + e^{22.9SN_1 - 5.51}}\right] \quad (4)$$

342 In the formula, SAN, SIL, CLA and C represent sand grains (0.05–2 mm), powder (0.002–
343 0.05 mm), clay (<0.002 mm) and organic carbon content (%), respectively; SN1=1-SAN/100.

344

345 3.2.3 Calculation of topographic factors in natural slope catchments

346 (1) Slope length factor

347 On the basis of the topographic map (1:2000 scale) and highway design of Xinhe Expressway,
348 the slope length factor of the slope catchment was calculated by using DEM data with 0.5 m
349 spatial resolution generated by ArcGIS. The natural slope catchment was divided into less than 1%,
350 1%–3%, 3%–5% and greater than or equal to 5% by using the 'reclassify' tool in ArcGIS. The *L*
351 factor algorithm of Moore and Burch (1986) was utilised in the operation formulas (Formulas (5)
352 and (6)).

353 $$L = \left(\frac{\lambda}{22.13}\right)^m \quad (5)$$

354 $$\lambda = flowacc \cdot cellsize, \quad (6)$$

355 where *L* is normalised to the amount of soil erosion along the slope length of 22.13 m, $\lambda$ is the
356 slope length, *flowacc* is the total number of contributing pixels for each pixel that is higher than
357 the pixel and cell size refers to the DEM resolution (0.5m). *m* is a variable length-slope exponent.
358 Formula (7) is expressed as

359 $$m = \begin{cases} 0.2 & \theta < 1\% \\ 0.3 & 1\% \le \theta < 3\% \\ 0.4 & 3\% \le \theta < 5\% \\ 0.5 & \theta \ge 5\% \end{cases} \quad (7)$$

where $\theta$ is the slope.

(2) Slope factor

The *S* factor was calculated as follows. If the slope was less than 18%, then the formula of McCool et al. (1987) was used. If the slope was greater than 18%, then the formula of Liu et al. (2000) was adopted. Formula (8) is expressed as

$$S = \begin{cases} 10.8 \cdot \sin\theta + 0.03 & \theta < 9\% \\ 16.8 \cdot \sin\theta - 0.05 & 9\% \le \theta < 18\% \\ 21.9 \cdot \sin\theta - 0.96 & \theta \ge 18\% \end{cases} \quad (8)$$

The DEM data were processed by ArcGIS to obtain slope data. The slope values of each prediction unit were extracted by using the Zonal statistics tool. With the classification tool in ArcGIS, the slope of the highway catchment of Xinhe was divided into less than 9%, 9%–18% and greater than or equal to 18%.

The *S* values of the slope catchments under the three slope grades were calculated by combining Formula (8) with ArcGIS techniques. The *LS* values of the slope prediction units are shown in Figure 7.

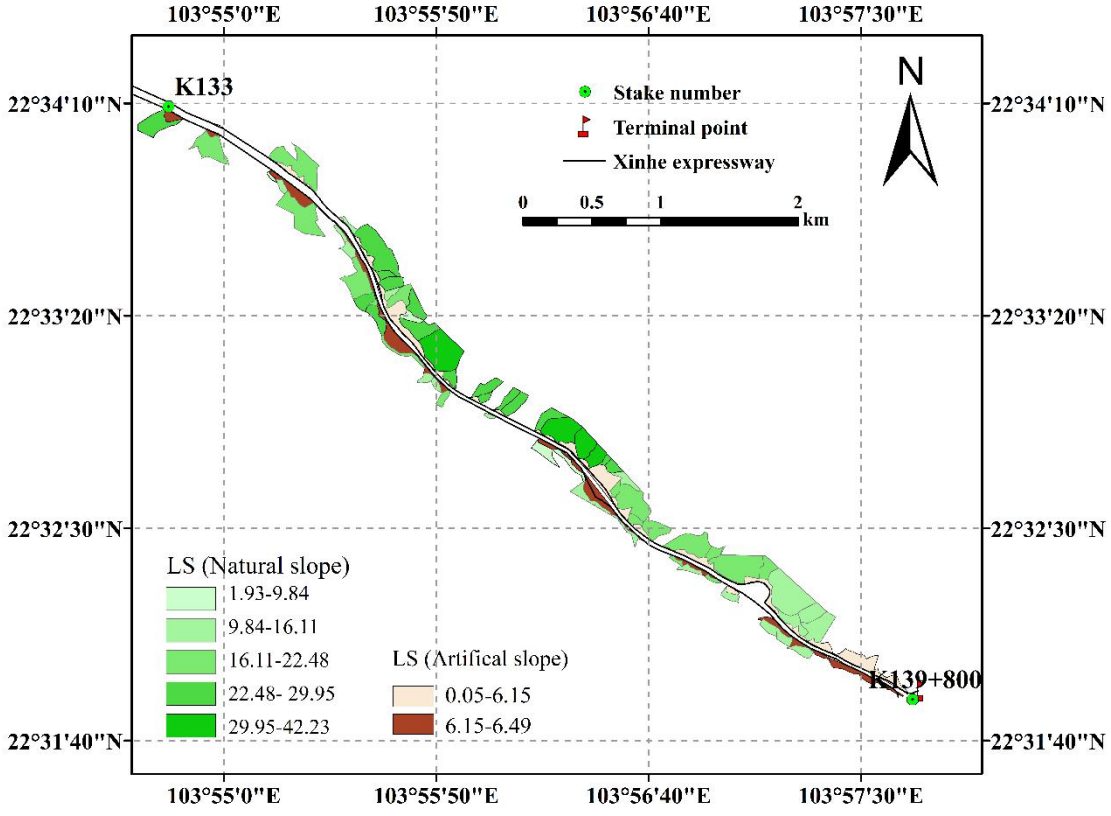


**Figure 7.** Spatial distribution map of topographic factors (K134–K139)

3.2.4 Calculation of topographic factors of artificial slopes

(1) Slope length factor

The method of Chen Zongwei (2010) was used for the calculation of the *LS* factor of the artificial slopes, and the calculation method for the topographic factors of the artificial slopes of Xinhe Expressway was modified. The slope length factor ($L_a$) was calculated using Formulas (5) and (6). The slope length index ($m_a$) was measured by conducting a runoff plot experiment and calculated using Formula (9).

$$m_a = log_{\frac{\lambda_1}{\lambda_2}} \frac{A_1}{A_2}, \quad (9)$$

where $A_1$ and $A_2$ are the soil erosion intensity values of two slopes when the slope lengths are $\lambda_1$ and $\lambda_2$, respectively (i.e. the specifications of the two slopes are the same except for slope length). The soil erosion amounts under 30 erosion rainfall conditions were monitored in the runoff field of Xiao Xinzhai in Mengzi City in 2014–2015 (Table 5). The $m_a$ value under each rainfall condition was calculated using Formula (9) according to the monitoring value of soil erosion amount. The average value of $m_a$ was 0.32, and it was regarded as the $m_a$ value of the artificial slope length factor (Table 6).

(2) Slope factor

The calculation of the slope factor was based on the method of Chen Zongwei (Chen et al., 2010). Six runoff plots were established in the Xiao Xinzhai runoff field of Mengzi City. Soil erosion intensity under the slope conditions of 1:1.5, 1:1.0 and 9:100 was monitored. Then, the slope factor for the slope condition was obtained using Formula (10).

$$S_\theta = \frac{A_\theta}{A}, \quad (10)$$

where $S_\theta$ represents the slope factor when the slope is $\theta$, $A_\theta$ represents the soil erosion intensity (t/ha), when the slope is $\theta$, and $A$ represents the soil erosion intensity (t/ha), when the slope is 9%. The three slope conditions (1:1.5, 1:1.0 and control slope of 9:100) in the soil erosion monitoring experiment were combined with Formula (10) to calculate the slope factor values of the two

slopes (1:1.5 and 1:1.0) under 30 rainfall conditions. The average factors of the slopes under the 1:1.5 and 1:1.0 slope conditions were 7.28 and 14.49, respectively (Table 7).

After the slope design drawings were digitised by ArcGIS, the slope and length values of each artificial slope prediction unit were determined according to design specifications. The slope length value of each artificial slope prediction unit was regarded as the horizontal projection length of the cement frame. The slope length of the six arris brick revetments was 0. Formulas (5), (6), (9) and (10), in combination with the slope length factor and $m_a$ and $S_\theta$ values, were used to calculate the value of *LS* of each artificial slope prediction unit.

**Table 7.** Calculation results of the slope factor

| The time of storm event or rainfall event | $S_{46}$ | $S_{56}$ |
|---|---|---|
| 2014.06.05 | 7.23 | 14.52 |
| 2014.06.07 | 7.25 | 14.47 |
| 2014.06.17 | 7.25 | 14.41 |
| 2014.06.28 | 7.33 | 14.62 |
| 2014.07.01 | 7.28 | 14.57 |
| 2014.07.13 | 7.27 | 14.57 |
| 2014.07.20 | 7.28 | 14.52 |
| 2014.08.02 | 7.20 | 14.43 |
| 2014.08.12 | 7.23 | 14.46 |
| 2014.08.26 | 7.27 | 14.60 |
| 2014.08.29 | 7.24 | 14.44 |
| 2014.09.02 | 7.25 | 14.56 |
| 2014.09.04 | 7.33 | 14.72 |
| 2014.09.17 | 7.30 | 14.32 |
| 2014.09.20 | 7.28 | 14.49 |

| | | |
|---|---|---|
| 2014.10.05 | 7.33 | 14.73 |
| 2015.07.04 | 7.23 | 14.36 |
| 2015.07.15 | 7.24 | 14.32 |
| 2015.07.24 | 7.17 | 14.15 |
| 2015.07.28 | 7.39 | 14.68 |
| 2015.08.13 | 7.28 | 14.47 |
| 2015.08.19 | 7.33 | 14.53 |
| 2015.08.26 | 7.35 | 14.47 |
| 2015.09.03 | 7.22 | 14.47 |
| 2015.09.12 | 7.28 | 14.47 |
| 2015.09.17 | 7.29 | 14.48 |
| 2015.09.25 | 7.28 | 14.47 |
| 2015.10.03 | 7.27 | 14.53 |
| 2015.10.08 | 7.36 | 14.71 |
| 2015.10.12 | 7.40 | 14.26 |
| Average | 7.28 | 14.49 |

*Note: Sxy represents the slope factor value simultaneously solved by erosion intensity values for monitoring plots numbered x and y.*

### 3.2.5 Cover and management practice factor

The *C* factor after topographic analysis is vital in soil loss risk control. In the RUSLE model, the *C* factor is used to depict the effects of vegetation cover and management practices on the soil erosion rate (Vander-Knijff et al., 2000; Prasannakumar et al., 2011; Alkharabsheh et al., 2013). The *C* factor is defined as the loss ratio of soils from cropped land under specific conditions to the corresponding loss from clean-tilled and continuous fallow (Wischmeier and Smith, 1978). Datasets from satellite remote sensing were initially used to assess the *C* factor due to the various land cover patterns with severe spatial and temporal variations mainly at the watershed scale (Vander-Knijff et al., 2000; Li et al., 2010; Chen et al., 2011; Alexakis et al., 2013). By taking full

advantage of NDVI data, $C$ was calculated according to the equation of Gutman and Ignatov (1998) (i.e. Formula (11)). Then, the vegetation coverage data were corrected by examining a sample plot every 2 km along the study area. The algorithm for calculating $f$ was adopted from the work of Tan et al. (2005) (i.e. Formula (11)). Finally, accurate vegetation coverage data were obtained (Figure 8). The $C$ factor map of the soil erosion prediction unit for the slope catchment area is shown in Figure 9.

$$C = 1 - \frac{NDVI - NDVI_{\min}}{NDVI_{\max} - NDVI_{\min}} \tag{11}$$

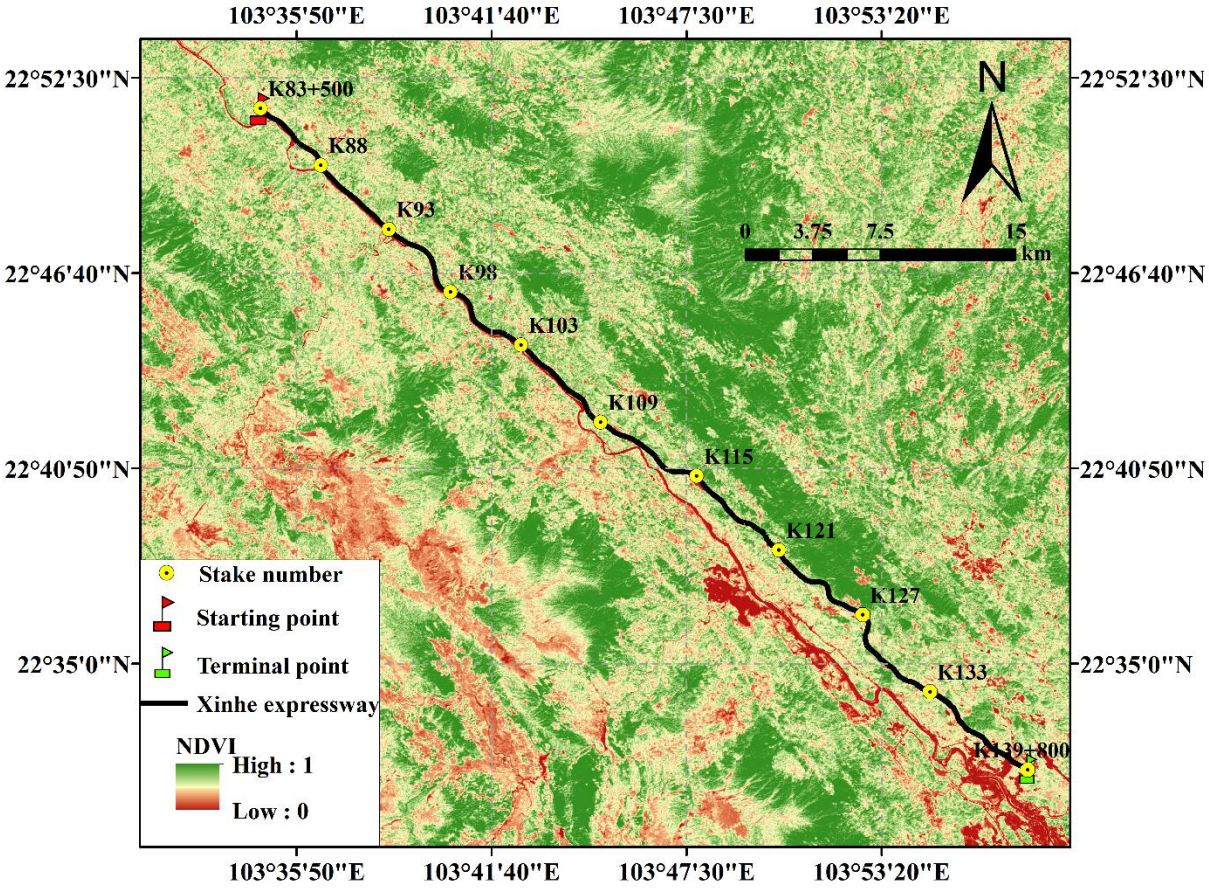


**Figure 8.** Vegetation coverage along Xinhe Expressway

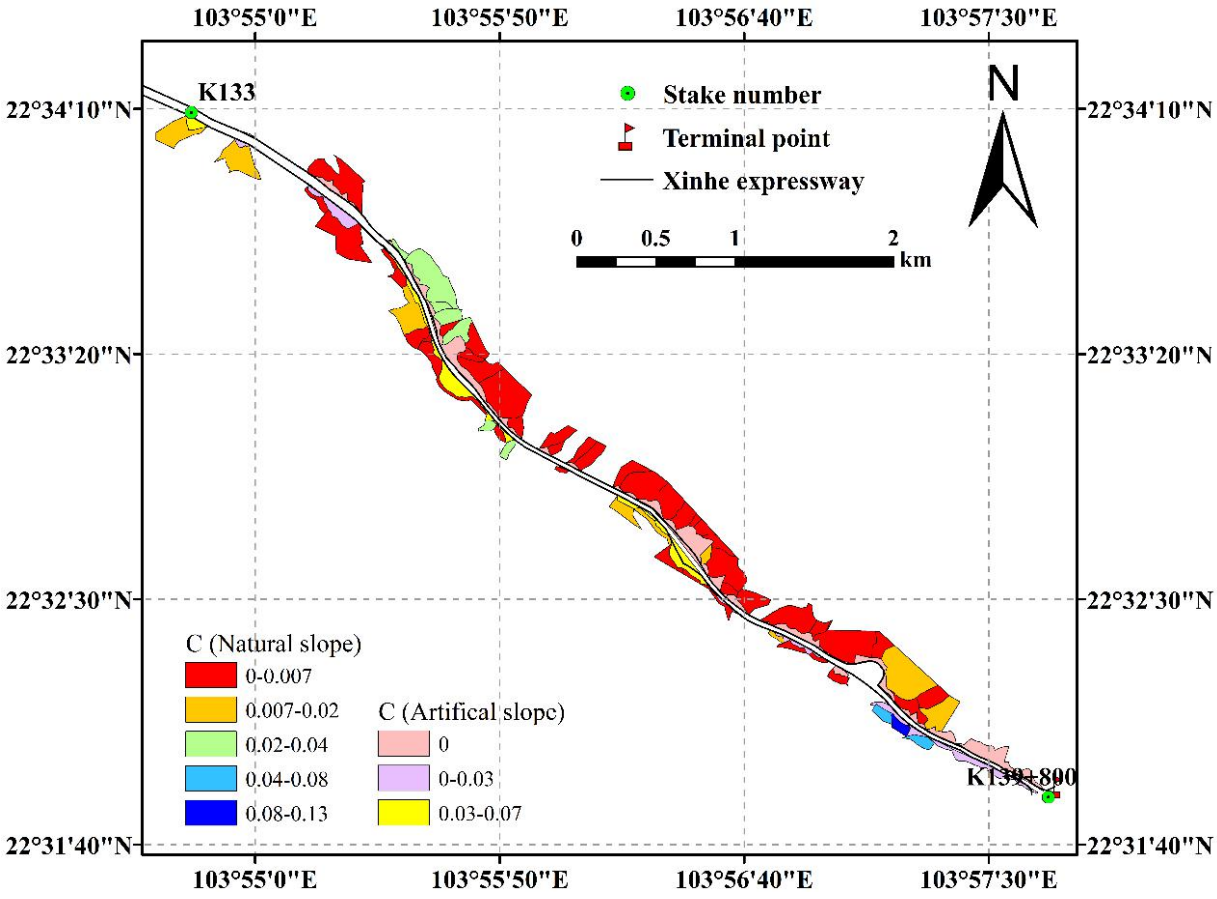


**Figure 9.** Spatial distribution map of the cover and management practice factor

### 3.2.6 Soil and water conservation measures

The land use types in the natural slope catchment area were classified as cultivated, forest, construction and difficult lands. Through a field investigation and visual judgment, the water conservation measures of farmland and forestland were identified as contour belt tillage, horizontal terrace and artificial slope catchment area, including cement frame and six arris brick revetments. The *P* values of the cement frame and the six arris brick revetments, which were determined by using the area ratio method, were 0.85 and 0.4, respectively. The *P* values of the soil and water conservation measures are shown in Table 8.

**Table 8.** *P* values of different slope types

| Slope type | Cement frame | Hexagonal brick | Contour strip tillage | Level bench/terrace | Construction land | Difficult to use land | Others |
|---|---|---|---|---|---|---|---|
| *P* | 0.85 | 0.4 | 0.55 | 0.03 | 0 | 0.2 | 1 |

### 3.3 Validation of model simulation accuracy

Soil erosion in three monitoring areas under 16 erosive rainfall conditions was monitored in 2014. No rainfall occurred in the 24 h before each rainfall event, and the disturbance of antecedent rainfall on soil erosion on the slopes was excluded. After estimating the historical soil loss of each slope prediction unit, the results were compared with data from the three monitoring plots along the side slope of Xinhe Expressway (Figures 10–12).

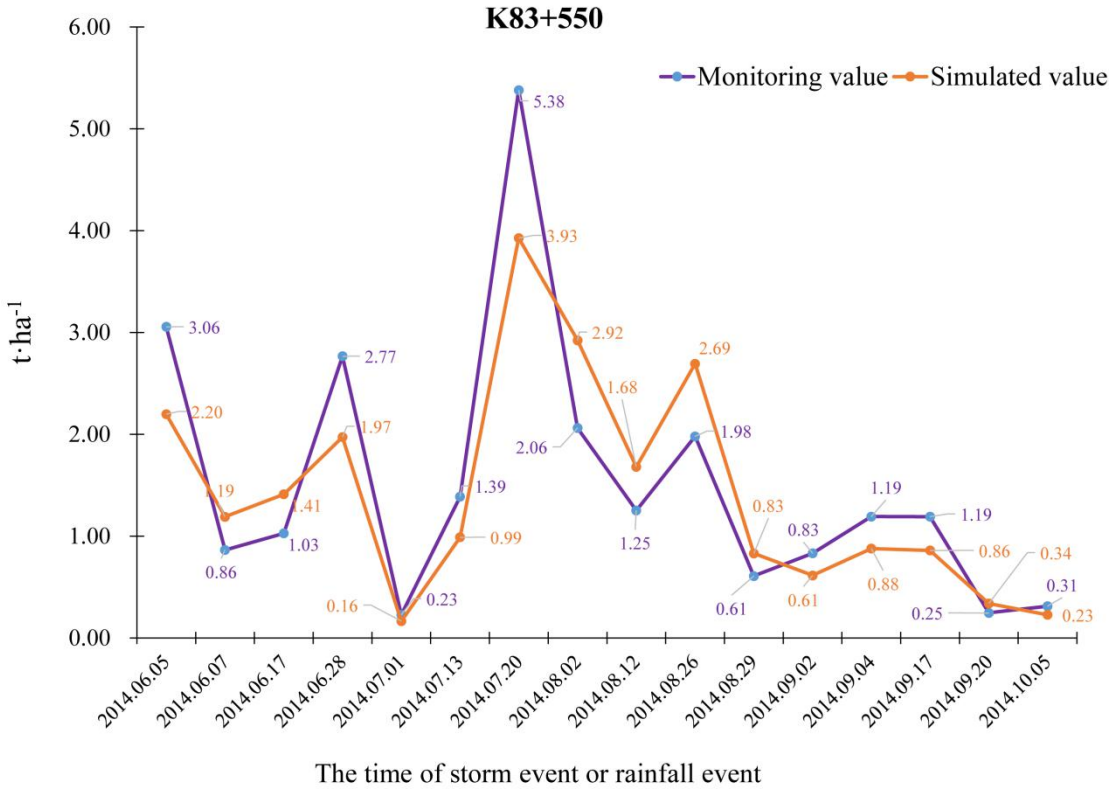


**Figure 10.** Comparison of model prediction and monitoring results (K83+550)

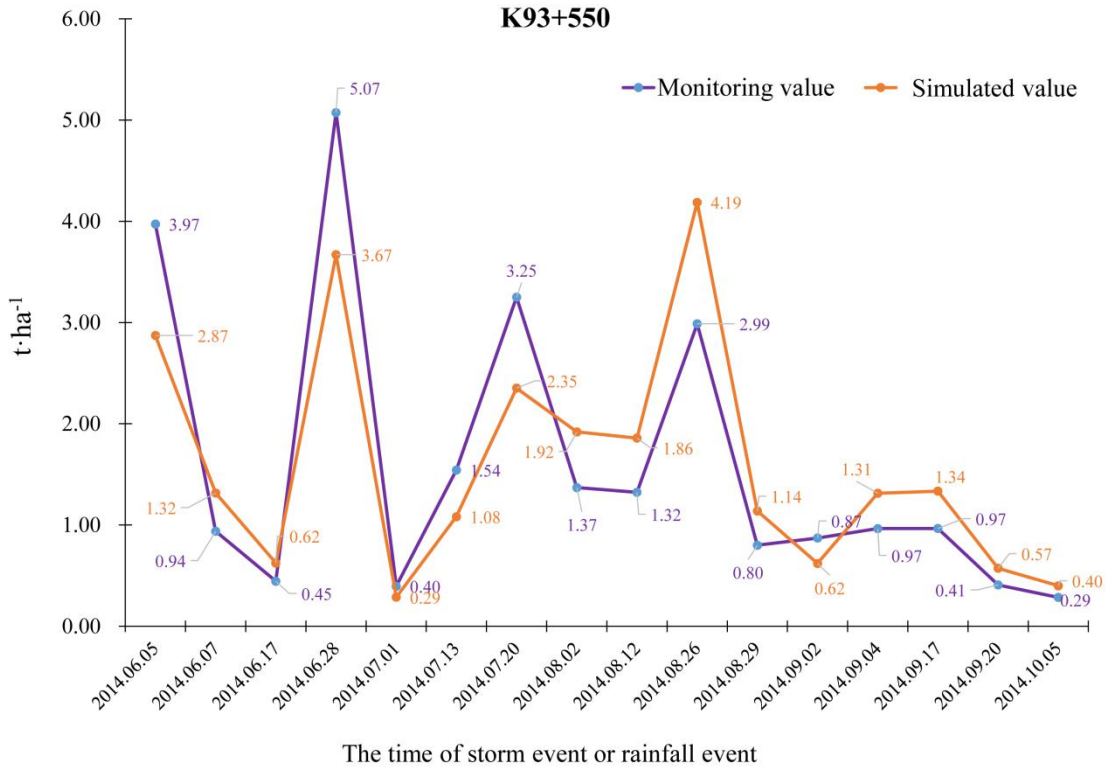


**Figure 11.** Comparison of model prediction and monitoring results (K93+550)

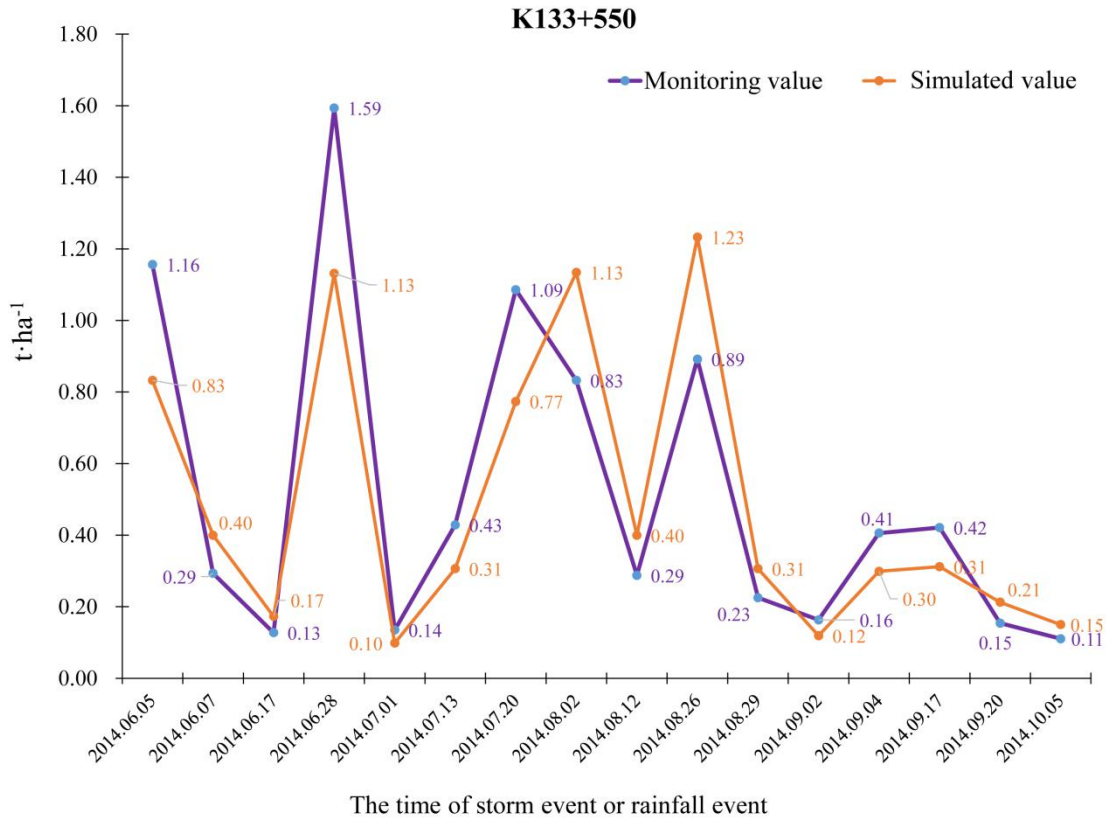


**Figure 12.** Comparison of model prediction and monitoring results (K133+550)

The error analysis showed that the absolute errors of the three monitoring areas under the 16 rainfall conditions were 0.47, 0.53 and 0.16 $t \cdot ha^{-1}$, and the overall average absolute error was 0.39 $t \cdot ha^{-1}$. The average relative errors were 31.80%, 35.49% and 32.26%, and the overall mean relative error was 31.18%. The root mean square errors were 0.59 0.66, and 0.21, all of which were within the acceptable range. The Nash efficiency coefficient of the model was 0.67, which is between 0 and 1, thereby showing that the model's accuracy satisfied the requirements. The calculation results are shown in Tables 10–12 (see supplementary material/appendices).

The northern and flat terrains of the southern region had a small simulation error because of the high and low areas of the central region of the terrain, which resulted in a slightly lower accuracy than that for the southern region. The absolute error of the simulation was large under heavy rainfall conditions. On the one hand, this result may be caused by the artificial error in sediment collection in the area. On the other hand, the model itself may be defective.

### 3.4 Application of early warning of soil erosion to the mountain expressway

The rainfall data and $I_{30}$ values in the 20 years covered by the study were obtained from the meteorological departments of Mengzi, Pingbian, Jinping and Hekou counties in Yunnan Province. Rainfall and its intensity were interpolated by co-kriging, which was introduced into the elevation and geographical position (Figures 13 and 14).

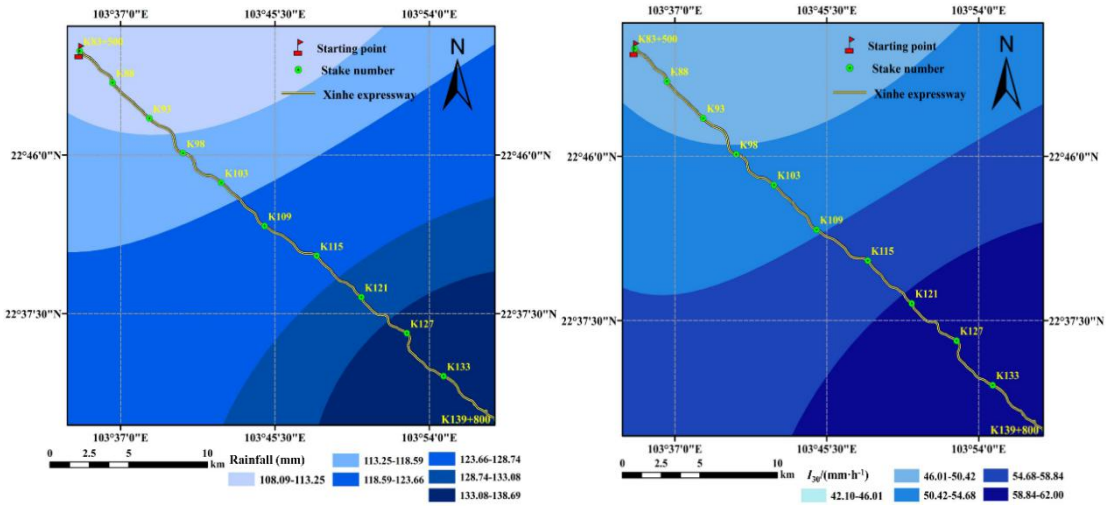


**Figure 13.** Rainfall interpolation results under 20-year return period

**Figure 14.** Rainfall intensity interpolation results under 20-year return period

The total soil erosion amount of each prediction unit for the 20-year return period rainfall data was obtained by simulation according to the classification standards of soil erosion intensity.

481 The prediction results were classified as ‘no risk’, ‘slight risk’, ‘moderate risk’, ‘high risk’ and
482 ‘extremely high risk’ (Figure 15(a) (b)).

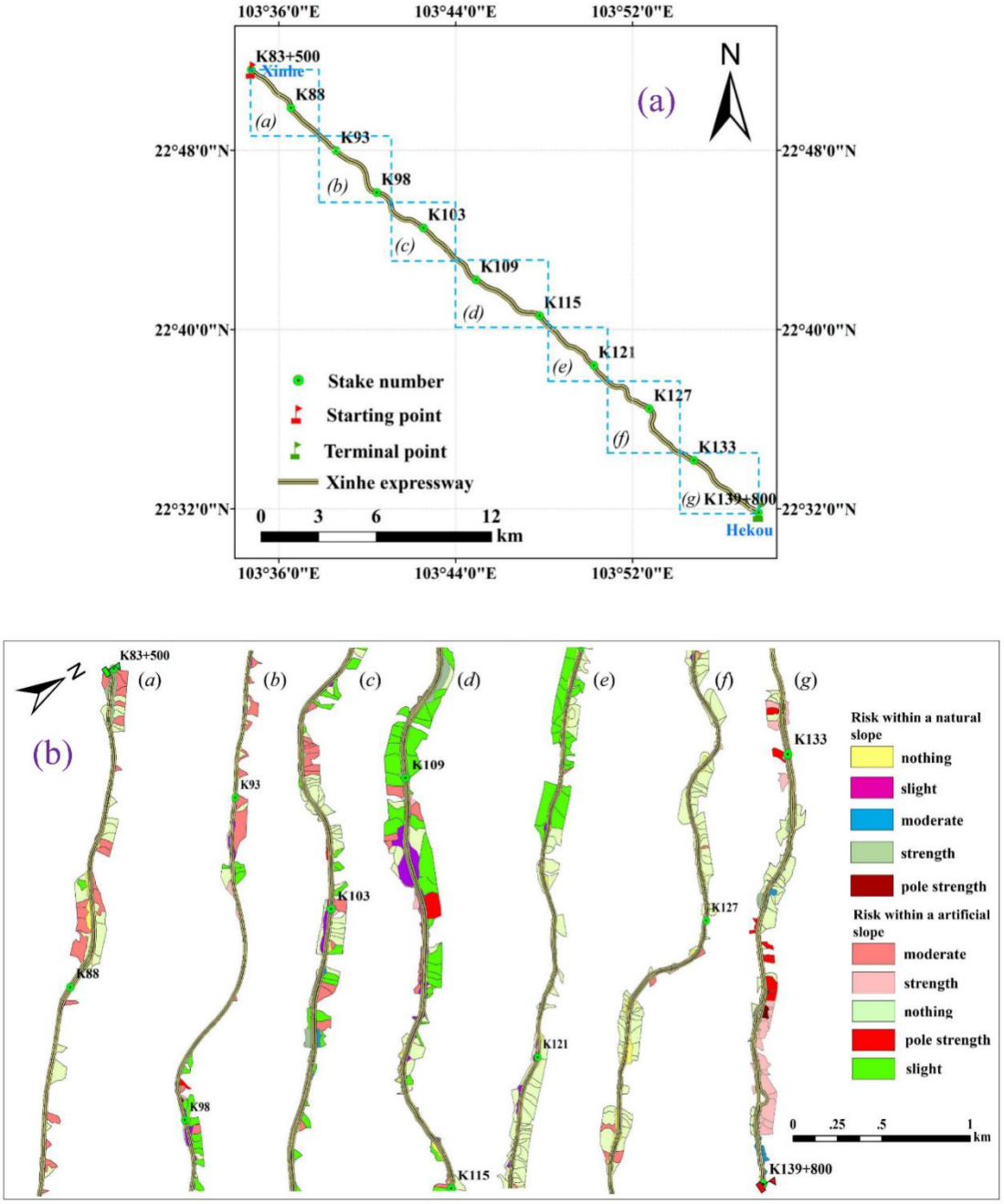


483
484 **Figure 15(a)(b).** Risk analysis of soil loss under 20-year return period rainfall conditions

485 The grading results showed that the percentage of prediction units classified as having low
486 and mild risks of soil loss was 88.60%. Given that the risk of soil erosion is low in these areas,
487 road traffic safety is not affected. The percentage of prediction units classified as having a
488 moderate risk was 4.29%. The risk of soil erosion in these areas is relatively low under general
489 rainfall intensity conditions. However, with high rainfall intensity, a certain scale of soil erosion
490 disaster could occur. The percentage of prediction units labelled as ‘high risk’ and ‘extremely high

risk' was 7.11%. The risk of soil erosion is high in these units. For example, from K134+500 to K135+500 (1000 m), the average soil erosion amount on both sides of the slope for the 20-year return period rainfall amount reached 17.57 t·ha$^{-1}$. Even if only a portion of the sediment is deposited on the road, road safety will still be affected.

Similarly, the risk of soil erosion was analysed according to the grading standard of soil loss risk under the 20-year return period rainfall condition. This analysis was performed by simulating the soil erosion amount of each prediction unit for the 1-year return period rainfall amount (Figure 16(a)(b)).

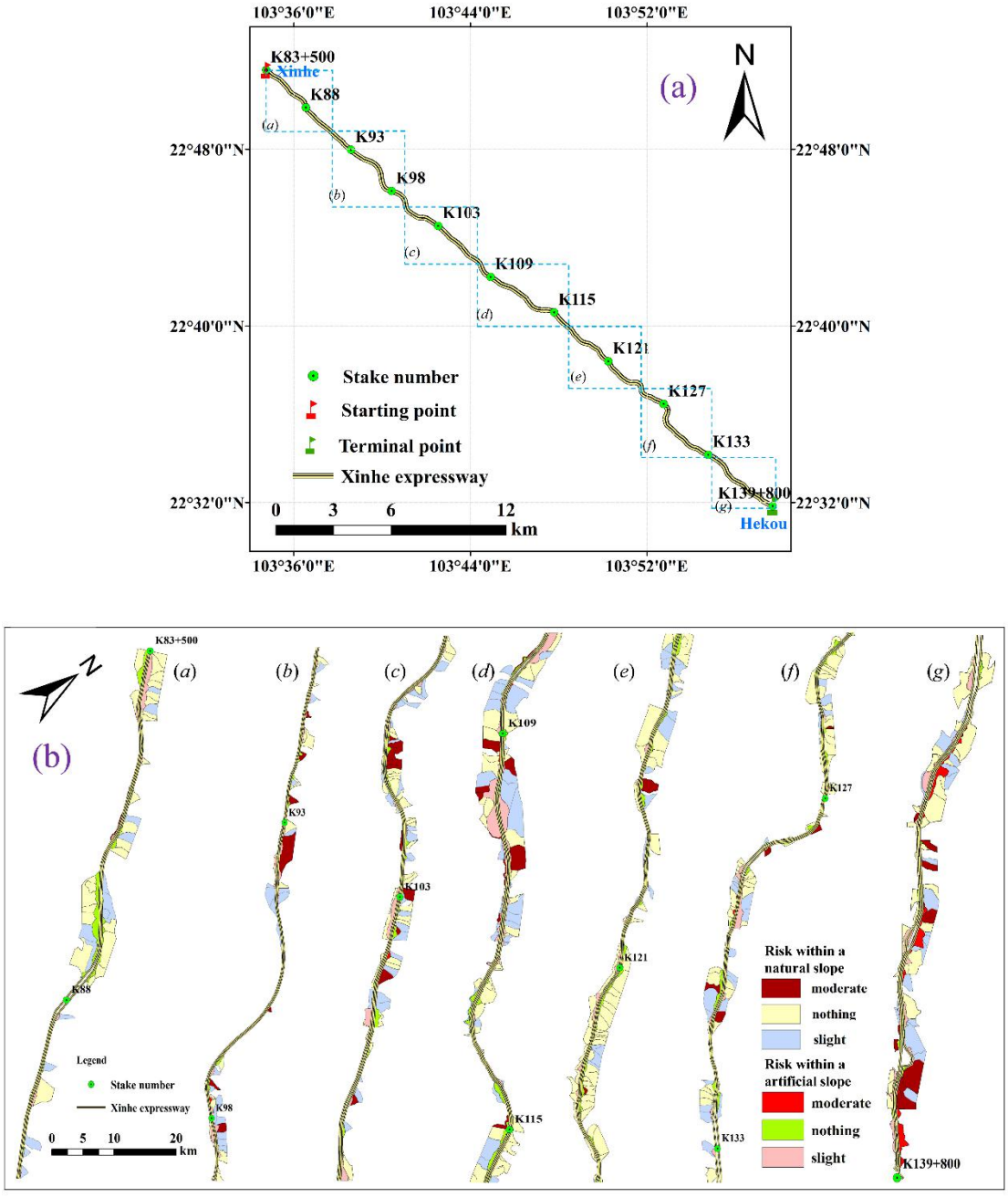


**Figure 16(a)(b).** Risk analysis of soil and water loss for the 1-year return period rainfall amount

The results indicated that the risk percentages of the prediction units for no soil erosion and mild soil erosion were 78.00% and 17.92%, respectively. Given that the risk of soil erosion is low in these areas, the safety of road traffic is not affected. The risk percentage of prediction units for mild soil erosion was 6.08%. Therefore, the layout of soil and water conservation measures in these areas should be rationally adjusted. Moreover, comprehensive management of their slopes should be strengthened, and plant and engineering measures should be applied comprehensively to conserve soil and water in these regions. Inspections must be reinforced, and motorists should be reminded to focus on traffic safety during rainy seasons. Most of the artificial slopes covered by the study area are made of six arris brick revetment; that is, the amount of soil erosion is small, and the frame-type cement slope protection against soil erosion is sturdier than those in other areas. Slope protection measures should be rationally adjusted according to the predicted results. We may adopt ecological slope protection technologies to slow down the roadbed slope and thus keep the slope stable. For example, the spraying and planting technology for bolt hanging nets can be used to build a layer of planting matrix that can grow and develop on the weathered rock slope because it can resist the porous and stable structure of the scouring. Technologies for masonry wall maintenance and honeycomb grid revetment protection can also be used. Various other technologies can be adopted to prevent and control soil erosion, and they can beautify the landscape environment of the road area whilst ensuring road traffic safety.

## 4 Discussion

Slope is the main factor of the soil loss caused by highways. Thus, slope is crucial for prediction and early warning systems. A highway slope can be divided into natural and engineering (artificial) slopes, and the RUSLE model can be used to predict soil erosion on natural slopes. Disregarding rainfall erosivity variations, we found that the methods of model parameter acquisition for literature analysis and for comparison of areas of the same type are consistent (Yang 1999; Yang 2002; Peng et al., 2007; Zhao et al., 2007; Chen et al., 2014; Zhu et al., 2016). After comparing the monitoring data with runoff plots, we discovered that the error between the predicted value and the monitoring value calculated by the RUSLE model is negligible (Yang 1999; Yang 2002; Li et al., 2004). These findings indicate that the prediction results of the model are reliable. In the prediction of erosion on engineering (artificial) slopes, previous studies emphasised surface disturbance during construction (He, 2004; Liu et al., 2011; He, 2008; Hu, 2016; Zhang et al., 2016; Song et al., 2007) but did not consider soil erosion as a result of the construction. In the process of predicting soil loss in engineering slopes by using the RUSLE model, the correction of the conservation support factor (i.e. cement block and hexagonal brick) is often ignored (Zhang, 2011; Morschel et al., 2004; Correa and Cruz, 2010). In addition, most

cases use RUSLE modelling to predict the soil erosion on highway slopes. Remote sensing is usually based on grid data and does not consider catchment units (IsIam et al., 2018; Villarreal et al., 2016; Wu and Yan 2014; Chen et al., 2010).

In this study, we analysed the characteristics of soil erosion during expressway construction to improve several aspects of previous research. First, we divided the highway slope into natural and artificial units and calculated the amount of soil loss from the slope surface to the pavement based on the slope surface catchment unit. Given that this approach is more in line with the actual situation than previous methods, the findings of the present study can be popularised. Second, we considered the spatial heterogeneity of the linear engineering of an expressway. The rainfall factor was spatially interpolated to compensate for the limitations on rainfall data, which were usually used by previous studies. Third, we modified the parameters of the artificial slope through an actual survey, runoff plot observation and other methods, and the parameters of the artificial slope were corrected by referring to the form of the project and the utilised materials.

## 5 Conclusions

In this study, we used the revised universal soil loss equation as the prediction model for soil loss on slopes, predicting the soil loss on highway slopes and simulating the risk of soil loss along the mountain expressway. We not only scientifically predict the amount of soil erosion caused by highway construction in mountain areas but also provide a scientific basis for the prevention and control of soil erosion and rational allocation of prevention and control measures. The error analysis of the actual observation data showed that the overall average absolute error of each monitoring area was 0.39 $t \cdot ha^{-1}$, the average relative error was 31.18%, the root mean square error was between 0.21 and 0.66 and the Nash efficiency coefficient was 0.67. The method of soil loss prediction adopted in this work generally has a smaller error and higher prediction accuracy than other models, and it can satisfy prediction requirements. The risk grades of soil loss along the slope of Xinhe Expressway were divided into 20- and 1-year return period rainfall conditions based on simulated predictions. The results showed that the percentage of slope areas with high and extremely high risks was 7.11%. These areas are mainly located in the K109+500–K110+500 and K133–K139+800 sections. Therefore, relevant departments should strengthen disaster prevention and reduction efforts and corresponding water and soil conservation initiatives in these areas.

## 6 Acknowledgment

This study was jointly supported by the Yunnan Provincial Communications Department Project (2012-272-(1)) and the Yunnan Provincial Science and Technology Commission Project (2014RA074).

## 7 References

Alexakis, D., Diofantos, G., Hadjimitsis, A.: Integrated use of remote sensing, GIS and precipitation data for the assessment of soil erosion rate in the catchment area of "Yialias" in Cyprus. Atmospheric Research, 131, 108-124, 2013.

Alkharabsheh, M.M., Alexandridis, T.K., Bilasb, G., Misopolinos, N.: Impact of land cover change on soil erosion hazard in northern Jordan using remote sensing and GIS. Four decades of progress in monitoring and modeling of processes in the soil-plant-atmosphere system: applications and challenges. Procedia Environmental Science, 19, 912-921, 2013.

Angulomartínez, M., and Beguería, S.: Estimating rainfall erosivity from daily precipitation records: a comparison among methods using data from the ebro basin (NE spain). Journal of Hydrology, 379(1): 111-121, 2009.

Bakr, N., Weindorf, D. C., Zhu, Y. D., Arceneaux, A. E., Selim, H. M.: Evaluation of compost/mulch as highway embankment erosion control in louisiana at the plotscale. Journal of Hydrology, s 468-469(6): 257-267, 2012.

Bosco, C., De Rigo, D., Dewitte, O., Poesen, J., and Panagos, P.: Modelling soil erosion at european scale: towards harmonization and reproducibility. Natural Hazards & Earth System Sciences, 2(4), 2639-2680, 2015.

Cai, C. F., Ding, S. W., Shi, Z. H., Huang, L., Zhang, G. Y.: Study of Applying USLE and Geographical Information System IDRISI to Predict Soil Erosion in Small Watershed. Journal of Soil and Water Conservation. 14(2): 19-24, 2000.

Chen, B. H.: The study on multivariate spatial interpolation method of precipitation in mountainous areas. Beijing Forestry University, 2016 (in Chinese).

Chen, F., Zeng, M. G., and Zhou, Z. H.: Evaluation for Ecological Benefits of Greening on Expressways in Mountainous Area. Technology of Highway and Transport, 1:139-143, 2015 (in Chinese).

Chen, S. X., Yang, X. H., Xiao, L. L., Cai, Y. H.: Study of Soil Erosion in the Southern Hillside Area of China Based on RUSLE Model. Resources Science, 36(6): 1288-1297, 2014 (in Chinese).

Chen, T., Niu, R. Q., Li, P. X., Zhang, L. P., Du, B.: Regional soil erosion risk mapping using RUSLE, GIS, and remote sensing: a case study in miyun watershed, north china. Environmental Earth Sciences, 63(3), 533-541, 2011.

Chen, Y. J., Sun, K. M., and Zhao, Y.: Experiment on the effect of rule caused by slope angle on sand and runoff under the condition of ecological protected slope. Journal of Water Resources & Water Engineering, 21(4):55-59, 2010 (in Chinese).

Chen, Z. W., He, F., and Wang, J. J.: Revises of Terrain Factors of Roadbed Side Slope in Universal Soil Loss Equation. HIGHWAY, 12:180-185, 2010 (in Chinese).

609 Chen, Z. W., He, F., and Wang, J. J.: Revises of Terrain Factors of Roadbed Side Slope in
610 Universal Soil Loss Equation. HIGHWAY, 12:180-185, 2010 (in Chinese)

611 Chen, Z. W., He, F., Wang, J. J.: Revises of Terrain Factor of Roadbed Side Slope in Universal
612 Soil Loss Equation. HIGHWAY, (12):180-185, 2010 (in Chinese).

613 China.com.cn.: The total mileage of road was 4,773,500km, the total mileage of highways was
614 136,500 km in China [EB/OL].
615 http://www.chinahighway.com/news/2018/1183657.php?tdsourcetag=s_pcqq_aiomsg, 2018-
616 08-24.

617 Correa, C. M. C., Cruz, J.: Real and estimative erosion through RUSLE from forest roads in
618 undulated at heavily undulated relief. Revista Árvore, 34(4): 587-595, 2010.

619 Cunha, E. R. D., Bacani, V. M., Panachuki, E.: Modeling soil erosion using RUSLE and GIS in a
620 watershed occupied by rural settlement in the Brazilian Cerrado. Natural Hazards, 85, 1-18,
621 2017.

622 Dong, H., Zeng, H.: Discussion on the current situation and the future of China highway
623 construction. Technology & Economy in Areas of Communication (TEAC), 5(3):17-18, 2003
624 (in Chinese).

625 Fei, X. H., Song, Q. H., Zhang, Y. P., Liu, Y. T., Sha, L. Q., Yu, G. R., Zhang, L. M., Duan, C. Q.,
626 Deng, Y., Wu, C. S., Lu, Z. Y., Luo, K., Chen, A. G., Xu, K., Liu, W. W., Huang, H., Jin, Y. Q.,
627 Zhou, R. W., Grace, J.: Carbon exchanges and their responses to temperature and
628 precipitation in forest ecosystems in Yunnan, Southwest China. Science of The Total
629 Environment, 616: 824-840, 2017.

630 Feng, Q., and Zhao, W. W.: The study on cover-management factor in USLE and RUSLE: a
631 review. ACTA ECOLOGICA SINICA, 34(16):4461-4472, 2014 (in Chinese).

632 Fenta, A. A., Yasuda, H., Shimizu, K., Haregeweyn, N., and Negussie, A.: Dynamics of Soil
633 Erosion as Influenced by Watershed Management Practices: A Case Study of the Agula
634 Watershed in the Semi-Arid Highlands of Northern Ethiopia. Environmental Management,
635 58(5): 1-17, 2016.

636 Foster, G. R., Weesies, G. A., McCool, D. K., Joder, D. C., Renard, K. G.: Revised Universal Soil
637 Loss Equation User's Manual. Gov. Print. Office, Washington D.C. (48p), 1999.

638 Gong, J., and Yang, P.: Study on the Layout of Soil and Water Conservation Monitoring Sites
639 during the Construction of Mountain Highways-Case Study of Enlai, Enqian Highway.
640 Subtropical Soil and Water Conservation, 28(1):9-11, 2016 (in Chinese).

641 He, F.: Prediction of soil erosion in foundation slope of South Hubei Road Based on RUSLE.
642 Beijing Normal University, 2008 (in Chinese).

643 He, X. W.: Study on prediction of soil erosion in Road area. Beijing Normal University, 2004 (in
644 Chinese).

645 Hu, L.: Study on development and mechanism of water Erosion and Ecological water erosion
646 control technology of Highway slope in Cold Region. Xi'an University of technology, 2016
647 (in Chinese).

Islam, M. R., Wan, Z. W. J., Lai, S. H., Osman, N., Din, M. A. M., Zuki, F. M.: Soil erosion assessment on hillslope of GCE using RUSLE model. Journal of Earth System Science, 127(4): 50, 2018.

Jia, Y. H., Dai, D. C., Liu, Y.: Performance Analyse and Evaluation of Freeway in China. JOURNAL OF BEIJING JIAOTONG UNIVERSITY, 29(6):1-5, 2005 (in Chinese)

Jia, Z. R., Guo, and Z. Y.: Quantifying Evalution Approach to Highway Soil Bioengineering. Research of Soil and Water Conservation, 15(2):260-262, 2008 (in Chinese).

Jiang, M., Pan, X. Y., Nie, W. T.: Preliminary analysis of prevention and control of soil and water loss in expressway project construction. Yangtze River, 48(12):61-64, 2017 (in Chinese).

Kateb, H. E., Zhang, H. F., Zhang, P. C., Mosandl, R. Soil erosion and surface runoff on different vegetation covers and slope gradients: A field experiment in Southern Shaanxi Province, China. Catena, 105(5): 1-10, 2013.

Kateb, H. E., Zhang, H. F., Zhang, P. C., Mosandl, R. Soil erosion and surface runoff on different vegetation covers and slope gradients: A field experiment in Southern Shaanxi Province, China. Catena, 105(5): 1-10, 2013.

Kinnell, P. I. A.: Applying the RUSLE and the USLE-M on hillslopes where runoff production during an erosion event is spatially variable. Journal of Hydrology, 519:3328-3337, 2014.

Li, H., Chen, X. L., Kyoung, J. L., Cai, X. B., Myung S.: Assessment of soil erosion and sediment

Li, J. G., Dao, H. Y., Zhang, L., Zhang, H. K.: Soil and Water Loss Monitoring in the Dianchi Watershed. Research of Soil and Water Conservation, 11(2): 75-77, 2004 (in Chinese).

Li, Y., Qi S., Cheng, B. H., Ma, J. M., Ma, C., Qiu, Y. D., Chen, Q. Y.: A Study on Factors of Space-time Distributions of Precipitation in Ailao Mountain Area and Comparison of Interpolation Methods. EARTH AND ENVIRONMENT, 45(6): 600-610 (in Chinese)

Lin, H. L., Zheng, S. T., and Wang, X. L.: Soil erosion assessment based on the RUSLE model in the Three-Rivers Headwaters area, Qinghai-Tibetan Plateau, China. ACTA PRATACULTURAE SINICA, 26(7):11-22, 2017 (in Chinese)

Liu, B. Y., Nearing, M. A., Shi, P. J., and Jia, Z. W.: Slope length effects on soil loss for steep slopes. Soil Science Society of America Journal 64(5): 1759-1763, 2000.

Liu, J. T., Zhang, J. B.: Interpolation analysis of the spatial distribution of precipitation in mountain area. Journal of Irrigation & Drainage, 25:34-38, 2006 (in Chinese)

Liu, S. L., Zhang, Z. L., Zhao, Q. H., Deng, L., Dong, S. K.: Effects of Road on Landscape Pattern and Soil Erosion: A Case Study of Fengqing County, Southwest China. Chinese Journal of Soil Science, 42(1): 169-173, 2011 (in Chinese).

Liu, W. Y.: Preliminary Study on *R* Index of Zhaotong Basin. Yunnan Forestry Science and Technology, (2):24-26, 1999 (in Chinese)

Liu, X. Y.: Study on the slope stability and its rheological influence in Mountain highway. Central South University, 2013 (in Chinese).

Liu, Z. Y., Zhang, X., Fang, R. H. Analysis of spatial interpolation methods to precipitation in Yulin based on DEM. Journal of Northwest A&F University (Nat. Sci. Ed.), 38:227-234,

2010 (in Chinese)

Mccool, D. K., Brown, L. C., Foster, G. R., Mutchler, C. K., and Meyer, L. D.: Revised slope steepness factor for the universal soil loss equation. Transactions of the ASAE-American Society of Agricultural Engineers (USA), 30(5): 1387-1396, 1987.

Millward, A. A., and Mersey, J. E.: Adapting the rusle to model soil erosion potential in a mountainous tropical watershed. Catena 38(2):109-129, 1999.

Molla, T., and Sisheber, B.: Estimating soil erosion risk and evaluating erosion control measures for soil conservation planning at Koga watershed in the highlands of Ethiopia. Solid Earth, 8, 1-23, 2017

Moore, I. D., and Burch, G. J.: Physical basis of the length-slope factor in the universal soil loss equation. Soil Science Society of America Journal, 50(5): 1294-1298, 1986.

Mori, A., Subramanian, S. S., Ishikawa, T., Komatsu, M. A Case Study of a Cut Slope Failure Influenced by Snowmelt and Rainfall. Procedia Engineering, 189: 533-538, 2017.

Mori, A., Subramanian, S. S., Ishikawa, T., Komatsu, M. A Case Study of a Cut Slope Failure Influenced by Snowmelt and Rainfall. Procedia Engineering, 189: 533-538, 2017.

Morschel, J., Fox, D. M., & Bruno, J. F.: Limiting sediment deposition on roadways: topographic controls on vulnerable roads and cost analysis of planting grass buffer strips. Environmental Science & Policy, 7(1): 39-45, 2004.

Mountain Region of Yunnan Province. SCIENTIA GEOGRAPHICA SINICA, 19(3):265-270, 1999 (in Chinese)

Panagos, P., Ballabio, C., Borrelli, P., Meusburger, K., Klik, A., Rousseva, S., Tadi´c, M.P., Michaelides, S., Hrabalíková, M., Olsen, P., Aalto, J., Lakatos, M., Rymszewicz, A., Dumitrescu, A., Beguería, S., Alewell, C.: Rainfall erosivity in Europe. Science of the Total Environment, 511:801-814, 2015.

Panagos, P., Borrelli, P., Meusburger, K., Yu, B., Klik, A., Lim, K.J., Yang, J.E., Ni, J., Miao, C., Chattopadhyay, N., Sadeghi, S.H., Hazbavi, Z., Zabihi, M., Larionov, G.A., Krasnov, S.F., Gorobets, A.V., Levi, Y., Erpul, G., Birkel, C., Hoyos, N., Naipal, V., Oliveira, P.T.S., Bonilla, C.A., Meddi, M., Nel, W., Al Dashti, H., Boni, M., Diodato, N., Van Oost, K., Nearing, M., Ballabio, C. Global rainfall erosivity assessment based on high-temporal resolution rainfall records. Scientific Reports, 7(1): 4175, 2017.

Panagos, P., Standardi, G., Borrelli, P., Lugato, E., Montanarella, L., Bosello, F.: Cost of agricultural productivity loss due to soil erosion in the European union: from direct cost evaluation approaches to the use of macroeconomic models. Land Degradation & Development. 2018.

Panos, P., Cristiano, B., Pasquale, B., Katrin, M., Andreas, K., Svetla, R., Melita, P. T., Silas, M., Michaela, H., Preben, O., Juha, A., Mónika, L., Anna, R., Alexandru, D., Santiago, B., and Christine, A.: Rainfall erosivity in Europe. Science of the Total Environment, 511: 801, 2015.

Peng, J., Li, D. D., Zhang, Y. Q.: Analysis of Spatial Characteristics of Soil Erosion in Mountain Areas of Northwestern Yunnan Based on GIS and RUSLE. Journal of mountain science, 25(5): 548-556, 2007 (in Chinese).

Prasannakumar, R., Shiny, N., Geetha, H., Vijith, H.: Spatial prediction of soil erosion risk by remote sensing, GIS and RUSLE approach: a case study of Siruvani river watershed in Attapady valley, Kerala, India. Environmental Earth Science, 965-972, 2011.

Renard, K. G., Foster, G. R., Weesies, G. A., Mccool, D. K, and Yoder, D. C.: Predicting soil erosion by water: a guide to conservation planning with the revised universal soil loss equation (RUSLE). Agriculture Handbook, 1997.

Renard, K. G., Foster, G. R., Weesies, G. A., McCool, D. K., Yoder, D. C.: Predicting soil erosion by water-a guide to conservation planning with the Revised Universal Soil Loss Equation (RUSLE). United States Department of Agriculture, Agricultural Research Service (USDA-ARS) Handbook No.703. United States Government Printing Office: Washington, DC. 1997.

Rick, D., Van, R., Matthew, E. H., and Robert J. H.: Estimating the LS Factor for RUSLE through Iterative Slope Length Processing of Digital Elevation Data within Arclnfo Grid. Cartography, 30(1): 27-35, 2001.

Shamshad, A., Azhari, M. N., Isa, M. H., Hussin, W. M. A. W., and Parida, B. P.: Development of an appropriate procedure for estimation of RUSLE $EI_{30}$ index and preparation of erosivity maps for Pulau Penang in Peninsular Malaysia. Catena, 72(3): 423-432, 2008.

Sharpley, A. N., and Williams, J. R.: EPIC-erosion/productivity impact calculator: 2. User manual. Technical Bulletin-United States Department of Agriculture, 4(4): 206-207, 1990.

Shi, Z. H., Cai, C. F., Ding, S. W., Wang, T. W., and Chow, T. L.: Soil conservation planning at the small watershed level using RUSLE with GIS: a case study in the three gorge area of china. Catena, 55(1): 33-48, 2004.

Shu, Z. Y., Wang, J. Y., Gong, W., Lv, X. N., Yan, S Y., Cai, Y., Zhao, C. P.: Effects of compound management in citrus orchard on soil micro-aggregate fractal features and soil physical and chemical properties. Journal of Nanjing Forestry University (Natural Sciences Edition), 41(5): 92-98, 2017.

Silburn, D. M.: Hillslope runoff and erosion on duplex soils in grazing lands in semi-arid central Queensland. III. USLE erodibility (K factors) and cover-soil loss relationships. Soil Research, 49(49): 127-134, 2011.

Soil and Water Conservation Society. RUSLE user's guide. Soil and Water Cons. Soc. Ankeny, IA. 164pp, 1993.

Song, F. L., Ma, Y. H., Zhang, C. X., Yu, H. M., Hu, H. X., He, J. L., Huang, J. Y.: Research progress on greening substrate material of ecological protection of expressway-side slope. Science of Soil and Water Conservation, 6:57-61, 2008 (in Chinese).

Song, X. Q., Zhang, C. Y., Liu, J.: Formation of Soil and Water Loss and Its Characteristics in Development and Construction Projects. Bulletin of Soil and Water Conservation, 27(5): 108-113, 2007 (in Chinese).

Stanchi, S., Freppaz, M., Ceaglio, E., Maggioni, M., Meusburger, K., & Alewell, C., and Zanini, E.: Soil erosion in an avalanche release site (Valle d'Aosta: Italy): towards a winter factor for RUSLE in the Alps. Natural Hazards & Earth System Sciences, 14(7), 255-440, 2014.

Tan, B. X., Li, Z. Y., Wang, Y .H., Yu, P. T., Liu, L. B.: Estimation of Vegetation Coverage and Analysis of Soil Erosion Using Remote Sensing Data for Guishuihe Drainage Basin. Remote sensing technology and application. 20 (2): 215-220, 2005.

769 Tan, S. H., and Wang, Y. M.: Research Progress and Thinking of Bioengineering Techniques for
770 Slope Protection in Expressway. Research of Soil and Water Conservation, 11(3):81-84, 2004
771 (in Chinese).

772 Taye, G., Vanmaercke, M., Poesen, J., Wesemael, B. V., Tesfaye, S., Teka, D., et al.: Determining
773 RUSLE P-and C-factors for stone bunds and trenches in rangeland and cropland, North
774 Ethiopia. Land Degradation & Development, 29(5), 2017.

775 Toy, T. J., Foster, G. R., Renard, K. G.: Soil Erosion: Processes, Prediction, Measurement, and
776 Control. 2002

777 Tresch, S., Meusburger, K., and Alewell, C.: Influence of slope steepness on soil erosion
778 modelling with RUSLE, measured with rainfall simulations on subalpine slopes. Bulletin of
779 Hokkaido Prefectural Agricultural Experiment Stations, 1995.

780 Vander-Knijff, J.M., Jones, R.J.A., Montanarella, L.: Soil Erosion Risk Assessment in Europe
781 EUR 19044 EN. Office for Official Publications of the European Communities, Luxembourg.
782 34, 2000.

783 Villarreal, M. L., Webb, R. H., Norman, L. M., Psillas, J. L., Rosenberg, A. S., Carmichael, S.:
784 Modeling landscape-scale erosion potential related to vehicle disturbances along the USA-
785 Mexico border. Land Degradation & Development, 27(4): 1106-1121, 2016.

786 Wang, C. J.: Regional Impaction and Evolution of Express Way Networks in China. PROGRESS
787 IN GEOGRAPHY, 25(6):126-137, 2006 (in Chinese)

788 Wang, H. J., Yang, Y., and Wang, W. J.: Prediction of Soil Loss Quantity on Side Slope of Freeway
789 Construction: Amendments to Main Parameters of USLE. Journal of Wuhan University of
790 Technology (Transporatation Science & Engineering), 29(1):12-15, 2005 (in Chinese).
791 Wang, K., and Gao, Z. L.: Analysis of Bioengineering Technology for Slope Protection of
792 Expressway: Taking Expressway from Ankang to the Border of Shaanxi and Hubei as an
793 Example. Ecological Economy, 31(5):155-159, 2015 (in Chinese).

794 Wang, L. H., Ma, B., and Wu, F. Q.: Effects of wheat stubble on runoff, infiltration, and erosion of
795 farmland on the Loess Plateau, China, subjected to simulated rainfall. Solid Earth, 8(2), 1-28,
796 2017.

797 Wang, W. Z., and Jiao, J. Y.: Qutantitative Evaluation on Factors Influencing Soil Erosion in China.
798 Bulletin of Soil and Water Conservation, (st):1-20, 1996 (in Chinese).

799 Wang, W. Z., and Zhang, X. K.: Distribution of Rainfall Erosivity *R* Value in China. Journal of soil
800 erosion and soil conservation, 2(1): 7-18, 1995.

801 Wang, W. Z., Jiao, J. Y., Hao, X. P., Zhang, X. K., Lu, X. Q., Chen, F. Y., Wu, S. Y.: Study on
802 Rainfall Erosivity in China. Journal of Soil and Water Conservation, (4):7-18, 1995 (in
803 Chinese)

804 Wischmeier, W.H., Smith, D.D.: Predicting rainfall erosion losses: a guide to conservation
805 planning. In: USDA, Agriculture Handbook No. 537, Washington, DC, 1978.

806 Wischmerie, W. H., and Smith, D. D.: Predicting rainfall-erosion losses from cropland east of the
807 rocky mountains: a guide to conservation planning, 1965.

808 Wu, Y. L., Yan, L. J.: Impact of road on soil erosion risk pattern based on RUSLE and GIS: a case
809 study of Hangjinqu highway, Zhuji section. ACTA ECOLOGICA SINICA, 34(19):5659-5669,

2014 (in Chinese).

Xiao, P. Q., Shi, X. J., Chen, J. N., Wu, Q., Yang, J. F., Yang, C. X., and Wang, C. G.: Experimental Study on Protecting Speedway Slope Under Rainfall and Flow Scouring. Bulletin of Soil and Water Conservation, 24(1):16-18, 2004 (in Chinese).

Xu, X. L., Liu, W., Kong, Y. P., Zhang, K. L., Yu, B. F., Chen, J. D.: Runoff and water erosion on road side-slopes: Effects of rainfall characteristics and slope length. Transportation Research Part D: Transport and Environment, 14(7): 497-501, 2009.

Yang, X.: Deriving rusle cover factor from time-series fractional vegetation cover for hillslope erosion modelling in new south wales. Soil Research, 52(52): 253-261, 2014.

Yang, Y. C., Wang, M. Z., Xu, Y. Y., Wang, P. C., and Song, Z. P.: Prediction of Soil Erosion on Embankment Slope of Qinhuangdao-Shenyang Special Line for Passenger Trains. Journal of Soil and Water Conservation, 15(2):14-16, 2001(in Chinese).

Yang, Y., and Wang, K.: Discussions on the Side Slope Protection System For Expressway. Industrial Safety and Environmental Protection, 32(1):47-49, 2006 (in Chinese).

Yang, Z. S.: A Study on Erosive Force of Rainfall on Sloping Cultivated Land in the Northeast

Yang, Z. S.: Study on Soil Loss Equation in Jinsha River Basin of Yunnan Province. Journal of mountain science, 20: 3-11, 2002 (in Chinese).

Yang, Z. S.: Study on Soil Loss Equation of Cultivated Slopeland in Northeast Mountain Region of Yunnan Province. Bulletin of Soil and Water Conservation, (1): 1-9, 1999 (in Chinese).

yield in Liao watershed, Jiangxi Province, China, using USLE, GIS, and RS. Journal of Earth Science 2 (6), 941-953, 2010

Yoder, D. C., Foster, G. R., Renard, K. G., Weesies, G. A., and Mccool, D. K.: C-factor calculations in RUSLE. American Society of Agricultural Engineers. Meeting (USA), 1993.

Yuan, J. P.: Preliminary Study on Grade Scale of Soil Erosion Intensity. Bulletin of Soil and Water Conservation, 19(6):54-57, 1999 (in Chinese).

Zeng, C., Wang, S. J., Bai, X. Y., Li, Y. B., Tian, Y. C., Li, Y., Wu, L. H., and Luo, G. J. : Soil erosion evolution and spatial correlation analysis in a typical karst geomorphology using RUSLE with GIS. Solid Earth, 8(4), 1-26, 2017.

Zerihun, M., Mohammedyasin, M. S., Sewnet, D., Adem, A. A., & Lakew, M.: Assessment of soil erosion using RUSLE, GIS and remote sensing in NW Ethiopia. Geoderma Regional,12: 83-90, 2018.

Zerihun, M., Mohammedyasin, M. S., Sewnet, D., Adem, A. A., Lakew, M.: Assessment of soil erosion using RUSLE, GIS and remote sensing in NW Ethiopia. Geoderma Regional, 12, 83-90, 2018.

Zhang, D. S.: The calculation of urban soil erosion based on GIS-a case study of Wuhan City. Southwest University of M.S.Dissertation, 2011 (in Chinese).

Zhang, H., Liao, X. L., Zhai, T. L.: Evaluation of ecosystem service based on scenario simulation of land use in Yunnan Province. Physics and Chemistry of the Earth, Parts A/B/C. 2017.

Zhang, T., Jin, D. G., Dong, G. C., Lin, J., Tang, P., Li, L. P.: Monitoring Soil Erosion in Linear Production and Construction Project Areas Based on RUSLE-A Case Study of North Ring

Expressway in Ningbo City, Zhejiang Province. Bulletin of Soil and Water Conservation, 36(5): 131-135, 2016 (in Chinese).

Zhang, T., Jin, D. G., Tong, G. C., Lin, J., Tang, P., Li, L. P.: Monitoring Soil Erosion in Linear Production and Construction Project Areas Based on RUSLE - A Case Study of North Ring Expressway in Ningbo City, Zhejiang Province. Bulletin of Soil and Water Conservation, 36(5):131-135, 2016 (in Chinese).

Zhao, C. C., Ding, Y. J., Ye, B. S., Zhao, Q. D.: Spatial distribution of precipitation in Tianshan Mountains and its estimation. Advance in water science, 22:315-322, 2011 (in Chinese)

Zhao, L., Yuan, G. L., Zhang, Y., He, B., Liu, Z. H., Wang, Z. Y., Li, J.: The Amount of Soil Erosion in Baoxiang Watershed of Dianchi Lake Based on GIS and USLE. Bulletin of So il and Water Conservation, 27(3): 42-46, 2007 (in Chinese).

Zhou, F. C.: Highway Slope Ecological Protection Against Erosion Mechanism and Control Effect Research. Chongqing jiaotong university, 2010 (in Chinese).

Zhou, R. G., Zhong, L. D., Zhao, N. L., Fang, J., Chai, H., Jian, Z., Wei, L., Li. B.: The Development and Practice of China Highway Capacity Research. Transportation Research Procedia, 15: 14-25, 2016.

Zhou, R. G., Zhong, L. D., Zhao, N. L., Fang, J., Chai, H., Jian, Z., Wei, L., Li. B.: The Development and Practice of China Highway Capacity Research. Transportation Research Procedia, 15: 14-25, 2016.

Zhu, J., Li, Y. M., Jiang, D. M.: A Study on Soil Erosion in Alpine and Gorge Region Based on GIS and RUSLE Model-Taking Lushui County of Yunnan Province as an Example. Bulletin of Soil and Water Conservation, 36(3): 277-283, 2016 (in Chinese).

Zhu, S. Q., Lin, J. L., and Lin, W. L.: Preliminary Study on Effects of Expressway Construction on Side-Slope Soil Erosion in Mountainous Areas. Resources Science, 26(1):54-60, 2004 (in Chinese).

Zhuo, M. N., Li, D. Q., and Zheng, Y. J.: Study on Soil and Water Conservation Effect of Bioengineering Techniques for Slope Protection in Highway. Journal of Soil and Water Conservation, 20(1):164-167, 2006 (in Chinese).